On the microstructure of Polypropylene by Pyrolysis GC-MS

On the microstructure of Polypropylenes by Pyrolysis GC-MS

Maria Paola Luda [a*1], Riccardo Dall'Anese[a2]

[a]Dipartimento di Chimica, Università di Torino Via P. Giuria 7 10125 Torino

Corresponding author Maria Paola Luda mariapaola.luda@unito.it tel +39 011 6707556 fax +39 011 6707855

ABSTRACT. In this work the pyrolysis products of various Polypropylenes (PP) have been identified in terms of structure and isomerism. The different microstructure of Polypropylenes reflected in the pyrolysis products provides a fingerprint which can be used to asses the origin of the different polymers. The distinction amongst various PP was possible through the quantitative analysis of the main pyrolysis products: 1-alkene pentamers, hexamers and heptamers. After individuation and quantification of these products, a statistic study through the Principal Components Analysis allowed to separate syndio and atactic Polypropylenes as well as isotactic Polypropylenes of different origin. The results of this study can be used in various fields, for example in forensic and commdities analyses or in quality control.

Keywords: Polypropylene, Pyrolysis Products, Tacticity, Pyrolysis-GC-MS, and Principal Component Analysis

Introduction.

[1] affiliated to NIS, Nanostructures Interfaces and Surfaces- Università di Torino

[2] email r.dallanese@buzzilab.it

Pyrolysis is one of the affirming way of polymer feedstock recycling, recovering valuable products depending on the structure of the parent polymer. Conversely pyrolysis is a powerful method to reveal polymer microstructure by converting the macromolecular chains in smaller fragments which, identified by GC-MS, allows to reconstruct the parent polymer structure.

Polypropylene (PP) is one of the polymers of larger production in the world, used in a huge variety of items spanning from fibres, plastics, packaging and so on. As all vinyl polymers with a pendant group it presents stereo and regio regularity based on the orientation of the monomer at the insertion. The regio and steric order in the polymers is mainly driven by the catalyst and synthesis conditions. New PP catalysts are rather selective; however errors can be introduced in the configuration due either to the catalyst site or chain end control. Therefore a detailed description of the tacticity of polymer allows to separate the origin of the different materials, and the result can be used in various fields, for example in forensic or commodities analyses or in quality control.

The final properties of the PP depends on the microstructure, and notably the thermal properties [1]; some researchers such as Lopez Moya [2] and Gomez-Elvira[3] put in evidence the contribution of the microstructure on the pyrolysis of syndiotactic PP. Pyrolysis of isotactic PP was considered as potential source of α–ω telechelic oligomers [4].

Thermal degradation and pyrolysis of PP was extensively investigated: Kiang [5] stated that most of the degradation products can be accounted for by a mechanism involving random scission followed by intramolecular H transfer. Noffz [6] suggested that intramolecular transfer of secondary radicals played an important role in the degradation mechanism of PP and that PPs yielded different chromatograms according to the tacticity of the material; Tsuchiya [7] pointed to the existence of irregular monomer placement from resulting 2-methyl-1-hexene.

It was shown that the characteristic pattern of PP pyrogram was preserved also in PP wood composites, somewhat enhancing the amount of monomers and dimers [8]. Most of the studies on Py-CG-MS have been carried out by Pyrolysis-Hydrogenation GC (PyH): Sugimura [9] and Ohtani [10] studied the PP pyrolysis by PyH and observing the chromatographic profile noticed the presence of many isomeric oligomers derived from the possible combinations of the methyl group within the polymeric chain and from the possible isomerisation at the radical intermediates during the pyrolysis process, as previously suggested by Seeger [11]. Isomerisation during pyrolysis has been documented also by Tsuge [12] for other polymers than PP. Tsuge and Ohtani [13] assigned chromatographic peaks of saturated heptamers of empirical formula $C_{22}H_{46}$, some minor products of PyH which are claimed to better maintain the original stereoregularity.

Audisio [14] correlated the structure of tetramer pyrolysis fraction (without hydrogenation) with the tacticity of some PP. Eventually Kruse [15] modelled the PP pyrolysis at mechanistic level to predict the formation of low molecular weight products. Many reactions were taken in account: chain fission, radical recombination, intermolecular H abstraction, midchain and end chain β scission, 1→3, 1→4, 1→5, 1→6 end and mid H transfer, disproportionation. Kinetic data are also reported indicating that 1→5 transfer is the most favourite and that end chain radical transfer occurs much faster than midchain radical transfer. According to that mechanism, four kinds of possible end groups are envisaged in the degradation products, reported in Table B in additional information.

It should be pointed up that a successful characterization of microstructure through pyrolysis requires a comprehensive knowledge of the pyrolytic mechanisms and a detailed qualitative and quantitative analysis of the pyrolysis products. In this paper the resulting data were used in Principal Component Analysis (PCA) as method to confront and identify the origin of the different PP polymers.

1. **Materials.**

In the whole 9 different PPs were investigated, four of them were standard PPs from Sigma Aldrich , five were commercial PPs from various sources.

The standard samples were:

- An isotactic PP (Mn 166000 Mw 580000 MFI (230°C/2.16Kg) 0.5 g/10 min
- An isotactic PP (Mn 50000 Mw 190000 MFI (230°C/2.16Kg) 35g/10 min,
- A syndiotactic PP (Mn 54000 Mw 127000 MFI (230°C/2.16Kg) 4.5g/10 min, 93%syn)
- An atactic PP (Mn 3700 Mw 140000)

The commercial samples were:

- A high molecular weight PP (>500000, Valtec HL 001 D, Indelpro)
- Some staple fibres of Meraklon
- A PP textile (tissue-no-tissue)
- Some fibres collected from a trunk tapestry
- A high molecular weight PP from a food box,

All samples were uncoloured apart from the tissue-no-tissue and the trunk tapestry which contained 0.96 and 1.24% of carbon black respectively (thermogravimetric measurements, TGA)

2. **Methods**

Pyrolysis were performed on a Curie's Point Pyrolyzer (GSG Analytical, Fisher Curie-Point Pyrolyzer 1040 PSC) coupled with GC-MS (Agilent 6890 Series Plus GC System, coupled with quadrupole mass spectrometer Agilent 5973 Mass Selective Detector). The pyrolysis were carried out at 670°C for 15 s; a high temperature was chosen in order to reduce the effect of the weak links (irregular structures) and make the pyrolysis basically driven by the standard PP microstructure. The mass of the sample was about 1 mg. Py-GC-MS measurements were carried out using an Agilent HP-5MS column (30m×250μm×0.25μm) under He flow (1 ml/min) and a split ratio of 1:40. The heating program was as follows: 40°C for 2 minutes, heating at 15°C/min up to 320°C hold up to 25.67 minutes. The interval of mass detection was from m/z 29-500 in the range 0-15 minutes, and 29-800 in the range 15-25.67min. The pyrolysis chamber was purged with He for 120 s before pyrolysis started. To avoid condensation of the heavier degradation products on the walls of the pyrolysis chamber a surrounding temperature of 200°C was selected.

Py-GC-MS measurements were carried out in triplicate or quadruplicate on each sample to check the reproducibility.

Data were analyzed by PCA, (XSTAT software). Two attempts were performed; in the first one (First PCA) 16 variables corresponding to 1-alkenes degradation products were selected: the three main pentamers, the five main hexamers and the eight main heptamers, as better described below. Quantification was done by integrating peaks obtained extracting ion at m/z 111; in each pyrogram these data were normalized to 100. Table A in the additional information reports the values of the peaks areas calculated in this way in each single pyrogram.

The second attempt (second PCA), was carried out with the aim of reducing noise. The variables of the first PCA were reduced from 16 to 8, selecting the most significant ones in the first PCA on the basis of their loading.

3. Results and discussion

A typical pyrogram of PP is reported in Figure 1, which is clearly dominated by clusters of peaks. Amongst these trimers appear as a singlet, tetramers as a doublet, pentamers as a triplet, whereas hexamers and heptamers are multiplets. Trimers account for about 15-20% of the volatile, main clusters from tetramers to heptamers for 38-45% depending on the sample. MS spectra of major and some minor degradation products and their possible attribution are reported in additional information section (Table D in additional information section).

Components of each major clusters exhibit a pretty similar MS pattern; the typical mass spectra of cluster members are reported in Figure 2 for tetramers, pentamers, hexamers and heptamers. In particular all these MS spectra exhibit a loss of 56 a.m.u. from the molecular ion. According to the McLafferty rearrangement [16] (Scheme 1) these pattern can be attributed to 1-alkenes, in agreement also with attribution of ref. [17].

So the components of each cluster are 1-alkenes having the structure of Scheme 2. Because of the presence of pseudo asymmetric Cs various stereoisomers are possible, which generate the observed multiplets.

From C-C random cleavage of the PP main chain a secondary $(R2)_x$ and a primary radical $(R1)_y$ of various polymerization degree are generated. Other secondary radicals can be formed by β scission of midchain radicals formed by intermolecular transfer. According to literature [1, 2, 15] 1-alkenes are formed from back biting of secondary radicals (intramolecular transfer + β scission at the link, chain side, position). Successive back biting reactions on the radical R2 continuously shorten this radical. If β scission occurs at the right, end group side, position, saturated alkanes are formed; 1-alkenes and alkanes account for 63-75% of the total volatiles (Table C in additional

information section). Scheme 3 depicts this pattern of degradation and the major degradation products.

Intramolecular transfer such as 1→3, 1→4, 1→5 or 1→6 are proposed to form 1-alkenes; amongst these 1→5 is the preferred because of a much lower activation energy due to the favourable 6 centres intermediate (10.6-12 kcal mol^{-1} instead of 23.6-25 kcal mol^{-1} for 1→3 transfer) [15], a number of stepwise intramolecular transfers has been proposed for 1-alkenes higher oligomers formation. [11, 12, 15].

Figure 3 illustrates the most probable path of formation of oligomers via back biting from the R2 radical, were C^1 is the C originally bearing the unpaired electron.

As shown in Figure 3, tetramers and superior oligomers are formed by a stepwise back biting involving one (tetramers and pentamers) or two (hexamers and heptamers) radical intermediates at C^5 and/or C^9 which can give inversion at the time of H extraction resulting in different stereoisomers after β scission took place. By comparing the intensity of the peak clusters of Figure 1 with mechanism elucidated in Figure 3 it can be seen that products formed through only 1→5 transfer (pentamers, heptamers) are formed in a major amount in comparison to those also requiring 1→3 transfer (tetramers, hexamers).

The oligomers reflect the structure of the pristine polymer, for example the pentamers represent a sequence of three chiral atoms in the parent PP, with the possibility of inversion at C^5 during pyrolysis, as reported by Seeger [11] and Tsuge [12]; hexamers and heptamers respectively contain sequences of four and five chiral C with possible inversion at C^5 and C^9. Tetramers were not considered in statistical studies because they represent a sequence of only two chiral C, increasing the noise of the results, however results here on such fraction are strictly in agreement to those of Audisio [14].

Minor pyrolysis products are formed by less probable degradation mechanism (such as disproportionation, intermolecular transfer or back biting from primary radicals) as suggested in additional information section, Tables C and D.

Concerning the major pyrolysis products up to heptamers, the different diastereoisomers of each cluster can be described in term of meso and racemic forms. For different PPs the relative amount of the diastereoisomers in the cluster is characteristic of microstructure of parent PP which in turn mainly depends on the PP synthesis conditions. Inversion occurring during pyrolysis modify the original stereoisomeric sequence, which can be somewhat predicted because it takes place at well defined position (C^5 and/or C^9).

4.1 Identification of stereoisomers

The different number of chiral carbons depends on the length of oligomer (Scheme 2) which generate then a great number of diastereoisomers whose structures are expected to be the key for discriminating the origin of different materials. The number of possible isomeric structures are 2^n, where n is the number of chiral carbons present in the oligomer. However the number of peaks in the relative cluster was lower because of both a non optimal chromatographic separation and a formation of couple of specular images, not separable with the used GC column. The identification was based on the characteristics of elution related to spatial orientations of methyl groups of oligomers. As a matter of fact, the increment of racemic (r) form relative to meso form (m) produces an increment of the oligomers boiling temperature, and consequently, the increment of retention time [12, 13]. The profiles of pentamers, hexamers and heptamers of the main clusters for iso-, atactic and syn- PPs obtained by extracting the ion m/z 111 are reported in Tables 1, 2 and 3. This ion has been chosen through the observation of the mass spectra in Figure 2, because it is present in all spectra with nearly the same relative abundance and allows a reduction of the noise in the pyrograms.

The association of the peak of each oligomer with single diastereoisomers is also reported in Tables 1, 2 and 3 for pentamers, hexamers and heptamers respectively.

It can be seen that, in pentamers and hexamers the first isomer in each cluster (P1 and HX1 respectively) is the more abundant in iso- PP whereas the last peak (P3 and HX5 respectively) is the more abundant in syn-PP. Therefore in each cluster the first peak should be assigned to all meso isomer and the last peak to the all racemic isomer, whereas those in the middle should be assigned to the mixed forms. Concerning the heptamers, HP4 is the more abundant peak in iso-polymer; this can be explained by considering that HP4 can be obtained from an iso- sequence through inversion at C^9 or at C^5 during the pyrolysis. These results support the assignation of mixed forms based on the increment of the retention time with the number of racemic structures within the oligomer.

The notation adopted in the tables was illustrated in Scheme 4 for pentamers where S and U are the saturated and unsaturated terminals; C^1 is always the carbon atom originally bearing the unpaired electron in R2 and here included in the saturated terminal S. A similar notation was adopted for hexamers and heptamers.

To take in account inversion possibly occurring during pyrolysis at C^5 and C^9, fragments which can be converted each other in this way are grouped together under the same number reported in the edge of the Tables 1, 2 and 3.

Oligomers in P1 and P3 can be generated from the same parent structure (either iso- or syn- sequences) via C^5 inversion during pyrolysis, so they are ascribed to the same group (group 1). Similarly, the two unseparable diastereoisomers in P2 are principally generated from an atactic sequence either with or without inversion; inversion at $C^5$of each P2 structure during pyrolysis generates the enantiomer of the other, so peak P2 is ascribed to a different group (group 2). P2 is mainly related to an irregular – three units long- sequence produced during the synthesis and in effect it is more abundant in

atactic PP than in iso- or syn-PP. Moreover, considering pentamers only, the average amount of P2 in syn-PP is of 20.7% (Table A in additional information). Only one structural unit over the three in P2 is in irregular position, corresponding to an average 6.9% of atactic contribute, in agreement with the declared 93% syn- degree claimed by the supplier of syn- PP.

Referring to the hexamers of Table 2, pyrolysis of a four-units-long iso- or syn- sequences in the parent PP can generate the fragments in HX1, HX2, HX4 and HX5 peaks ascribed to group 1 because they all can be interchanged through C^5 and/or C^9 inversion during pyrolysis. However irregular structures would also appear in HX2 (one racemic structure) and HX4 (two racemic structures) which cannot be converted to those of group 1 via C^5 or C^9 (inversion at other C than C^5 or C^9 are required) but can instead be converted each other via C^5 or C^9 inversion during pyrolysis and so are ascribed to group 2. In addition it seems that atactic structures generates in pyrolysis fragments of group 2 in HX3. As it can be seen in Table 2, HX3 peak is more abundant in the atactic PP than in regular iso- or syn- PP. therefore it is possibly related to the irregular structures produced during the synthesis.

Based on the possibility of inversion at C^5 and C^9 during pyrolysis the heptamers can be divided into three groups. Five units iso- or syn- sequences in parent PP are able to generate fragments in HP1, HP4 and HP8 peaks (group 1). HP4 peak also contains fragments of the group 3 which also appear in HP5 peak. Whereas HP2, HP3, HP6 and HP7 peaks contains fragment of the atactic groups 2. So HP2, HP3, HP6 and HP7 peaks as well as HP5 are mainly related to the irregular sequences produced during the synthesis. In HP4 some atactic structure are contained together those coming out from predominant syn- or iso- sequences.

4.2 Quantitative analysis and Principal Component Analysis (PCA)

Quantification has been carried out on the 16 peaks of Tables 1, 2 and 3 (1-alkenes) using the Extracted Ion Chromatogram (EIC) on the ion at m/z 111. The calculated areas for each pyrogram were normalized at 100. Because pyrograms were replicated, 28 pyrograms for the 9 samples were investigated and data on each pyrogram are reported in Table A in additional Information section. Pentamers accounted for 46-53%, hexamers for 16-21% and heptamers for 25-32% depending on the sample.

These values have been statistically studied using PCA. In the first attempt (first PCA): the 16 variables previously described were considered and the results of the first PCA are reported in Figure.4.

F1 and F2 represent respectively 54.72% and 27.62% of the variance in the loadings plot (Figure 5): the atactic components HP2 HP3 and HP5 stay in the first quadrant (-1,1), the mainly syn- components HX5, HP8 and P3 exhibit negative F2 values whereas thee mainly iso- components HP1, HX1 and P1 have positive F1 values. However there is not an efficient separation amongst the different samples as shown by the scatter plot of Figure 4. Therefore a further attempt (second PCA) has been done by selecting some specific variables on the basis of the contribution of variance and of the loading value. The 8 selected variables are those in Figure 6 (high modulus and equally spaced in the plane F1-F2). In the second PCA F1 and F2 represent now 54.62% and 40.28% of the variance, as reported in the loadings plot (Figure 6). The scatter plot of the second PCA is reported in Figure 7; the contribution of each component to the variables is reported in Table 4.

A better separation of the clusters identifying the different materials has been obtained from the second PCA (Figure 7). Atactic PP and Syn PP appear well separated in quadrant 1 and 3 respectively. As expected HP2 and HP3 attributed chiefly to atactic oligomers have the major contribute in atactic PP. Isotactic and commercial samples are distributes mainly along the F1 axis. From the study of the contributions of variance of the components F1 and F2 (as reported in the Table 4) it is possible to

notice that isotactic form drives the polymer toward high positive F1 values in the scatter plot, so separation of the components on F1 can be imputed to the polymeric material's grade of isotacticity. On the other hand, the separation on F2 axis is linked to the syndiotactic (negative values) and atactic forms (positive values).

4. Conclusion

Pyrolysis of PP leads to a mixture of mainly to 1-alkenes of different length and stereoisomery, no matter the original structure of the parent polymer because of the possibility of inversion during the pyrolysis process. However the mixture differs on quantitative basis.

Production of mainly isotactic PP largely prevails over that of other isomers chains. The PP microstructure reflects the choice of the catalyst and of the synthesis condition and therefore a different microstructure reveals a different origin of the polymer. Pyrolysis is a powerful method of microstructure investigation having an analytical valence as a fingerprint of the parent polymer. Moreover, identification of pyrolysis products gives information on the structure of the pristine polymer provided that the mechanism of their formation is known. Knowing that and selecting the appropriate condition, pyrolysis can be redirected toward recovering of valuable products in feedstock recycling technologies.

High temperature pyrolysis of PP produces mainly 1-alkenes through intramolecular hydrogen transfer on secondary radicals. The isomerism of these products and their quantification allows a distinction between even similar PP provided that a statistical evaluation of data is performed. In effect the scatter plot reported in Figure 7 highlight a deep difference in the origin of the polymers analyzed and an efficient separation even of isotactic materials. This separation is possible because along the component F1 there is a separation based on the grade of isotacticity of the material, while along the

component F2 there is a separation linked to contribution of syndiotactic and atactic segments present in the sample. Molecular weight of the parent PP seems not to be of relevance in this respect. Therefore the research of simple thermal degradation products has permitted to separate effectively the origin of materials, exploiting a simple and rapid technique of analysis the results of which can be useful as a way to confront in many sectors of analysis. To further advance in the understanding of the factors driving such separation the GC-MS results will be next cross-checked with the characterization performed by using other techniques (FTIR, ^{13}C-NMR) and molecular weight (GPC, viscometry), which would allow ensuring the accuracy of the distinction among isotactic PP grades found on the F1 axis in the PCA analysis.

Bibliography

[1] He P, Xiao Y, Zhang P, Xing C, Zhua N, Zhu X, Yan D. Thermal degradation of syndiotactic polypropylene and the influence of stereoregularity on the thermal degradation behaviour by in situ FTIR spectroscopy. Polym Degrad Stabil 2005; 88:473-479

[2] López Moya E, Thelakkadan AS, Verde Sesto E, Gómez-Elvira JM. The role of microstructure in the pyrolysis of polypropylene. A preliminary study on the syndiotactic stereoisomer. Polym Degrad Stabil 2011; 96:1087-1096

[3] Gómez-Elvira JM, Benavente R, Martínez MC. Unravelling the contribution of chain microstructure in the mechanism of the syndiotactic polypropylene pyrolysis. Polym Degrad Stabil 2013; 98:1150-1163

[4] Sawaguchi T, Ikemura T, Seno M. Prepration of α,ω-Diisopropenyloligopropylene by thermal degradation of isotactic polypropylene. Macromolecules 1995; 24:7973-7978

[5]. Kiang JKY, Uden P., Chien JCW. Polymer reactions-part VII: Thermal pyrolysis of polypropylene. Polym Degrad Stabil 1980; 2:113-127

[6] Noffz D, Benz W, Pfab W. Untersuchung von hochpolymerenmittelspyrolyse-gas-chromatographie. Fresen Z Anal Chem 1968; 1:121-137

[7] TsuchiydaY, Sumi K. Thermal decomposition products of polypropylene. J Polym Sci A1 1969; 7:1599-1607

[8] Jakab E, Varhegyi G, Faix O. Thermal decomposition of polypropylene in the presence of wood-derived materials. J Anal Appl Pyrol 2000; 56:273-285

[9] Sugimura Y, Nagaya T, Tsuge S, Murata T, Takeda T. Microstructural characterization of polypropylenes by high-resolution pyrolysis-hydrogenation glass capillary gas chromatography. Macromolecules 1980; 13:928-932

[10] Ohtani H, Tsuge S, Ogawa T, Elias HG. Studies on stereospecific sequence distribution in polypropylenes by pyrolysis-hydrogenation fused-silica capillary gas chromatography. Macromolecules 1984; 17:465-473

[11] Seeger M, Cantow H. Thermischespaltungs mechanismen in homo- und copolymerenaus α-olefinen, 2.polypropylene mitbekanntertaktizität, polyisobutylen und poly(1-buten). Makromolekul Chem 1975; 176: 2059-2078

[12] Tsuge S, Ohtani H. Structural characterization of polymeric materials by pyrolysis. Polym Degrad Stabil 1997; 58:109-131

[13] Tsuge S, Ohtani H. in Applied pyrolysis handbook. Wampler TP. Ed,.CRC Press 2006

[14] Audisio G., Bajo G. Flash pyrolysis of poly(propylene) stereoisomers. Makromolekul Chem 1975; 176:991-998

[15] Kruse TM, Wong HW, Linda L, Broadbelt LL. Mechanistic modelling of polymer pyrolysis: Polypropylene. Macromolecules, 2003; 36:9594-9607

[16] McLafferty FW. Interpretation of mass spectra, Fourth Edition. University Science Book 1993

[17] Tsuge S, Ohtani H, Watanabe C. in Pyrolysis-GC-MS Data Book of Synthetic Polymers, Thermograms and MS of Pyrolyzates Elsevier, 2011

Captions to the figures

Figure 1: Typical pyrogram at 670°C of PP's sample. The major oligomers clusters formed in the pyrolysis process are reported.

Figure 2. Typical MS spectra of degradation products in the main clusters of Figure 1. tetramers (A), pentamers (B), hexamers(C) and heptamers(D).

Figure 3. Back biting from R2 and principal patterns of formation of different 1-alkenes from R2 radical

Figure 4: Scatter plot for first PCA (16 variables).

Figure 5: Loadings plot of the first PCA

Figure 6: Loadings plot of the second PCA.

Figure 7: Scatter plot of the second PCA.

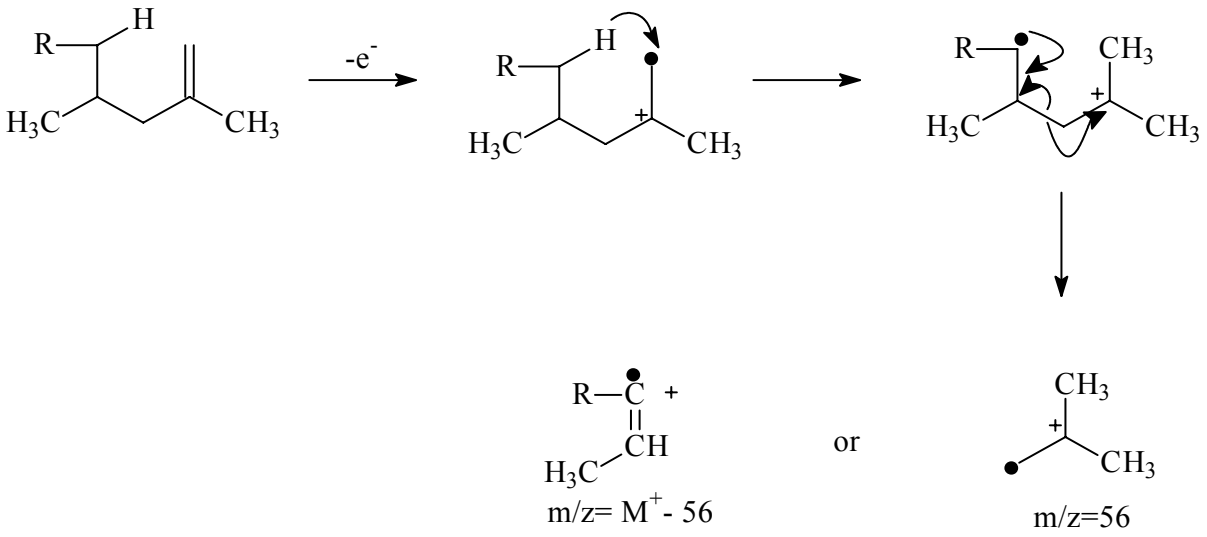

Scheme 1. Mc Lafferty rearrangement for 1-alkenes

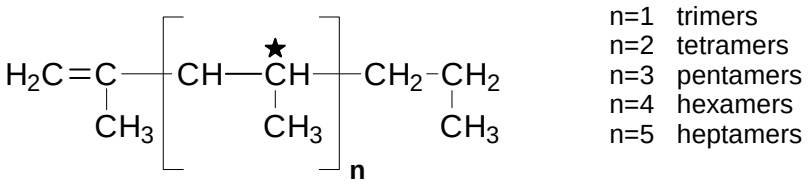

Scheme 2. Structure of various stereoisomers of the main cluster (* highlights pseudo asymmetric C)

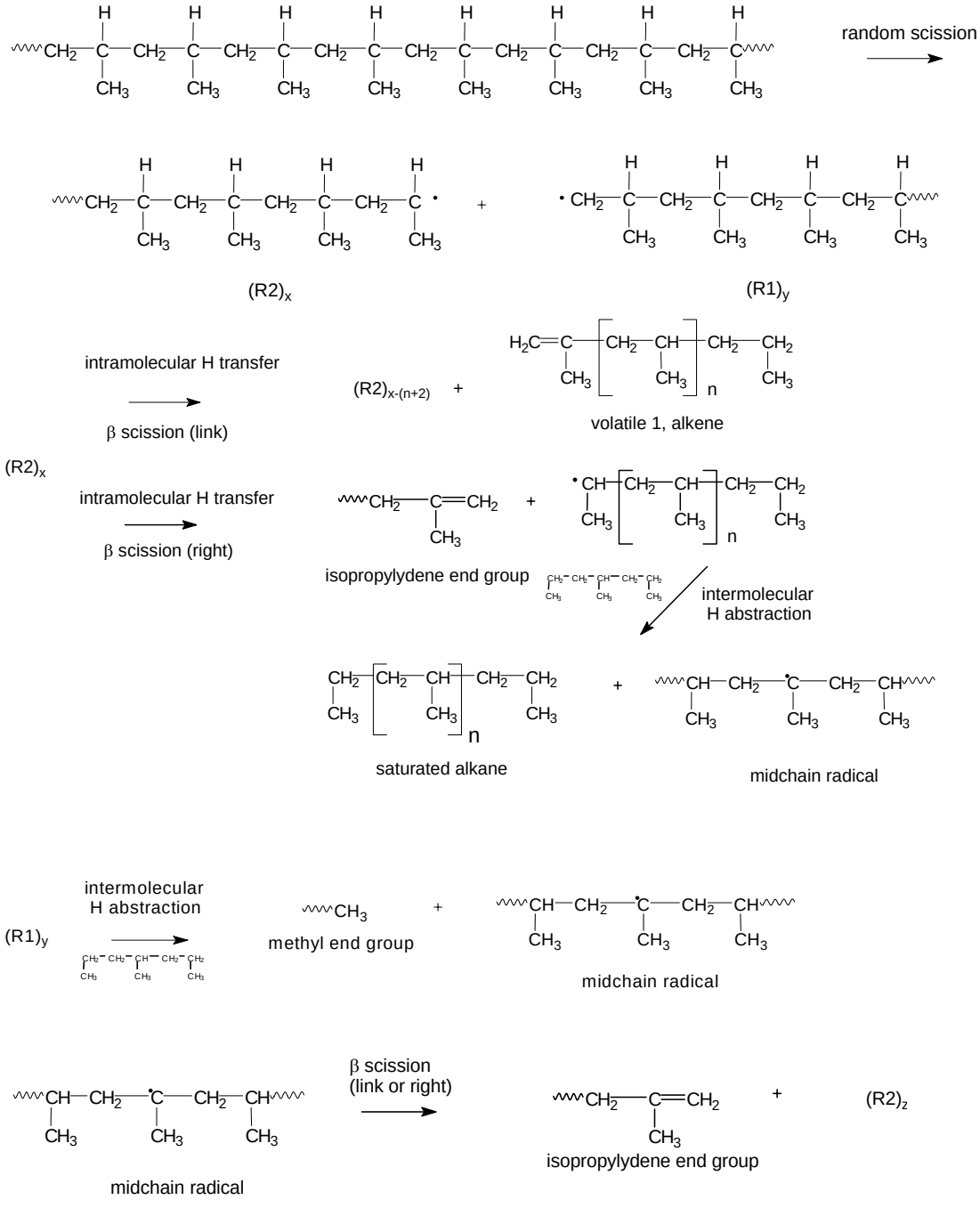

Scheme 3. Degradation pattern for PP explaining formation of the main degradation products (1-alkenes and alkane)

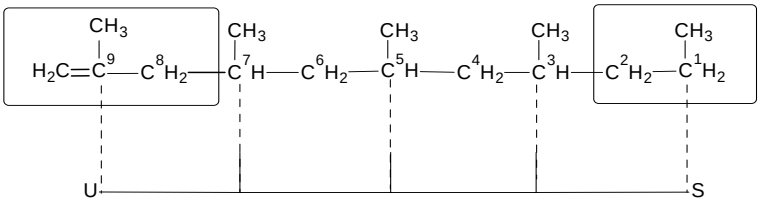

Scheme 4: notation adopted in the tables for pentamers: U and S are the unsaturated and saturated terminal, C^{1} is the C atom originally bearing the unpaired electron in R2

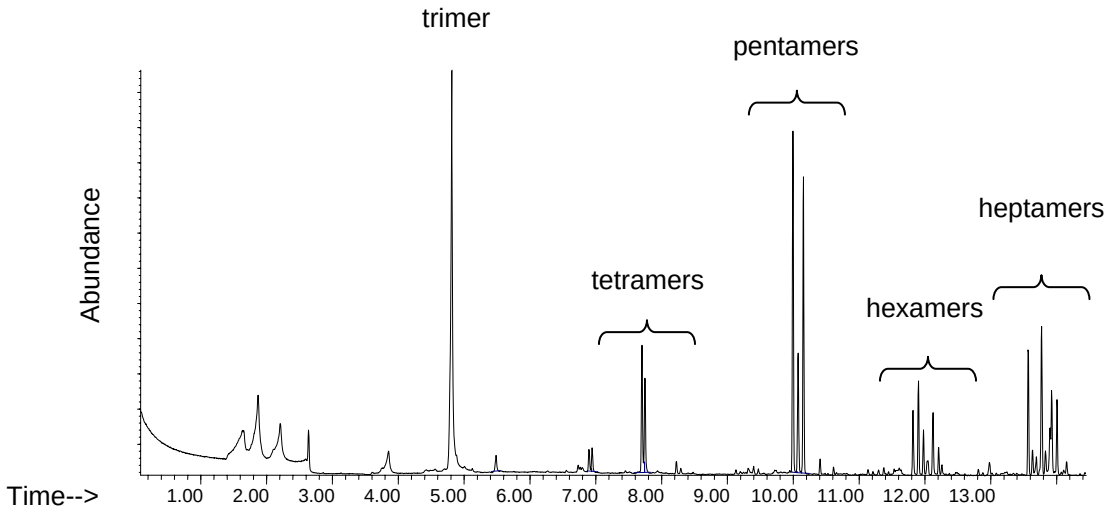
trimer
pentamers
heptamers
tetramers
hexamers
Abundance
Time-->
1.00
2.00
3.00
4.00
5.00
6.00
7.00
8.00
9.00
10.00
11.00
12.00
13.00

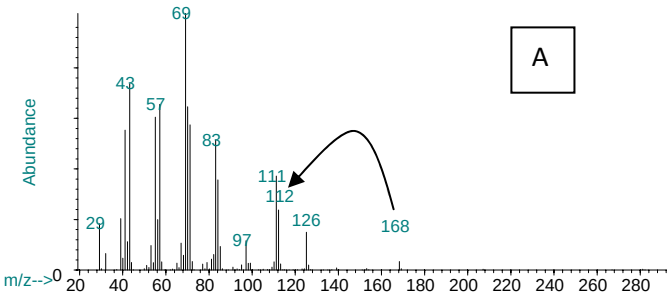
A
Abundance
m/z-->0
69
43
57
83
111
112
126
168
29
97
20 40 60 80 100 120 140 160 180 200 220 240 260 280

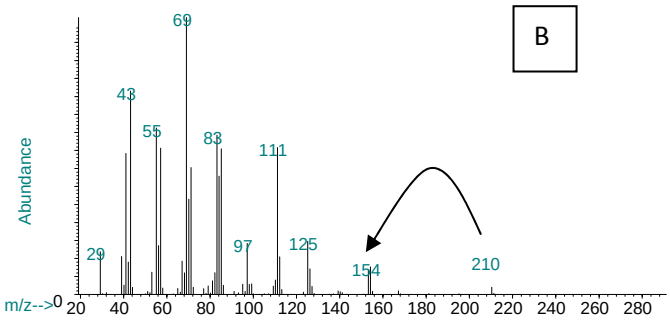
B
Abundance
m/z-->0
69
43
55
83
111
97
125
154
210
29
20 40 60 80 100 120 140 160 180 200 220 240 260 280

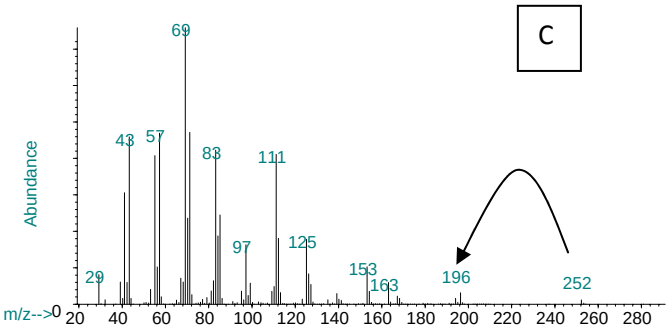
C
Abundance
m/z-->0
69
43
57
83
111
97
125
153
163
196
252
29
20 40 60 80 100 120 140 160 180 200 220 240 260 280

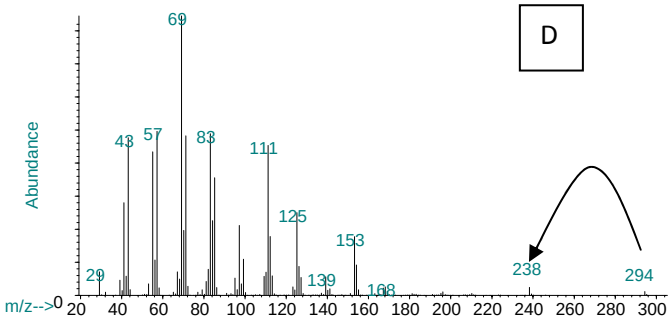
D
Abundance
m/z-->0
69
43
57
83
111
125
153
139
238
294
29
20 40 60 80 100 120 140 160 180 200 220 240 260 280 300

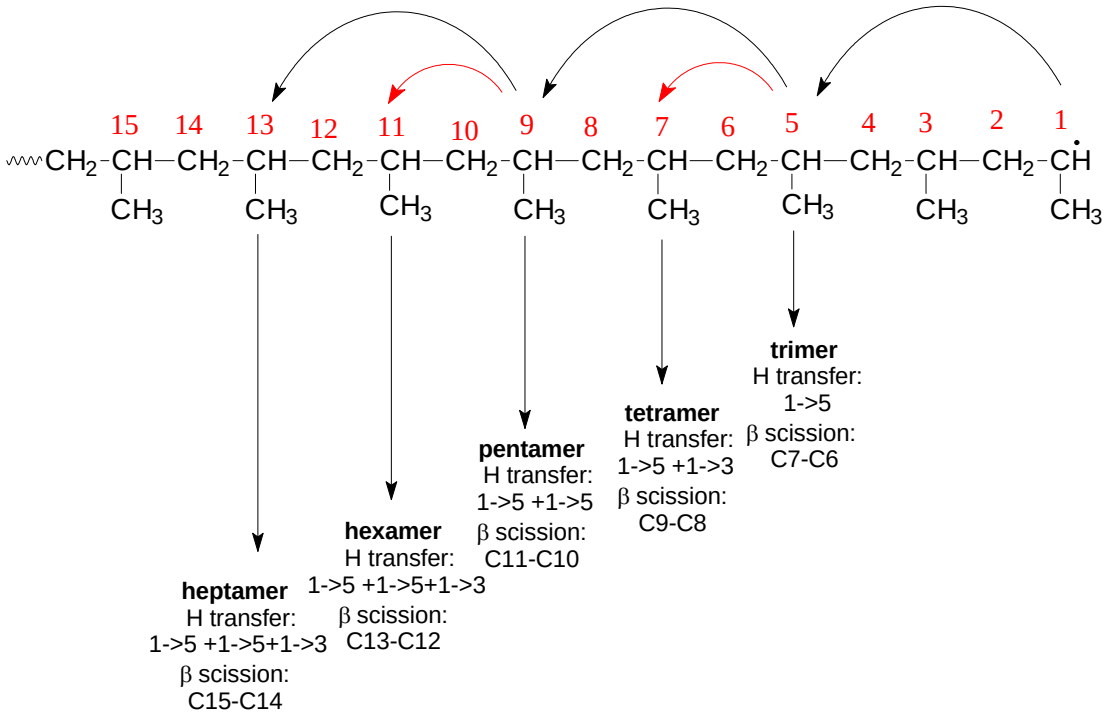
15 14 13 12 11 10 9 8 7 6 5 4 3 2 1
CH2-CH-CH2-CH-CH2-CH-CH2-CH-CH2-CH-CH2-CH-CH2-CH-CH2-CH-CH2-CH
CH3 CH3 CH3 CH3 CH3 CH3 CH3
heptamer
H transfer:
1->5 +1->5+1->3
β scission:
C15-C14
hexamer
H transfer:
1->5 +1->5+1->3
β scission:
C13-C12
pentamer
H transfer:
1->5 +1->5
β scission:
C11-C10
tetramer
H transfer:
1->5 +1->3
β scission:
C9-C8
trimer
H transfer:
1->5
β scission:
C7-C6

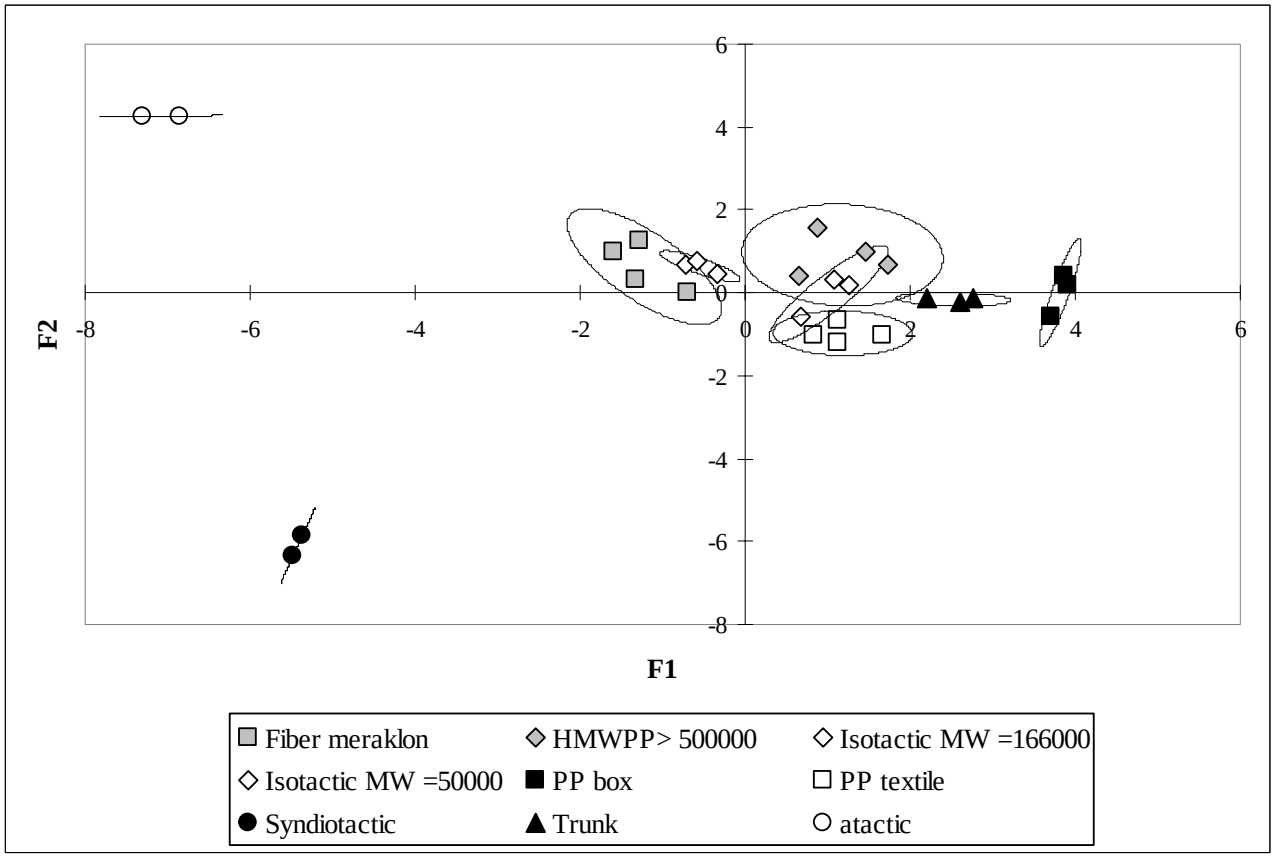
6
4
2
0
-2
-4
-6
-8
-8
-6
-4
-2
0
2
4
6
F2
F1
Fiber meraklon
HMWPP> 500000
Isotactic MW =166000
Isotactic MW =50000
PP box
PP textile
Syndiotactic
Trunk
atactic

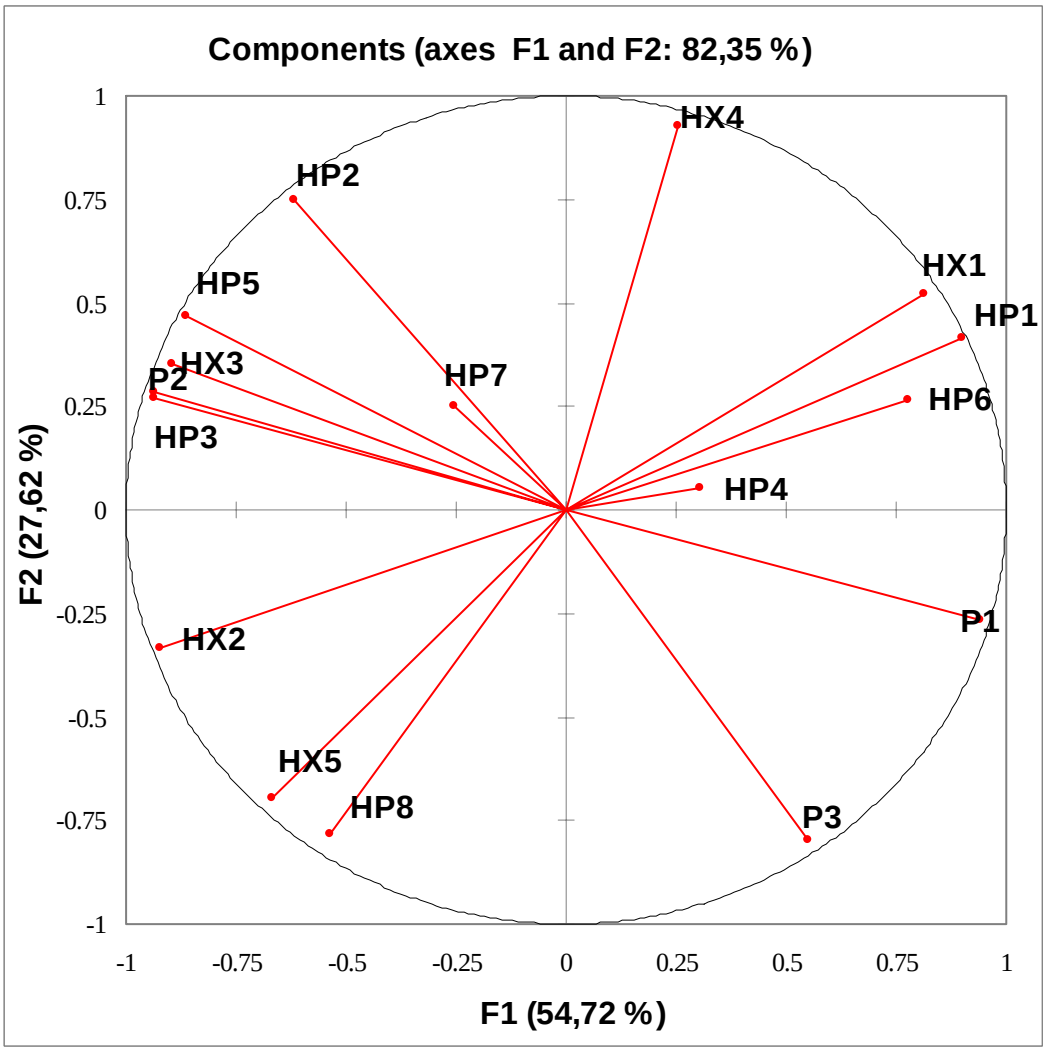
Components (axes F1 and F2: 82,35 %)
F2 (27,62 %)
F1 (54,72 %)
1
0.75
0.5
0.25
0
-0.25
-0.5
-0.75
-1
-1
-0.75
-0.5
-0.25
0
0.25
0.5
0.75
1
HX4
HP2
HX1
HP1
HP5
HX3
P2
HP7
HP6
HP3
HP4
P1
HX2
HX5
HP8
P3

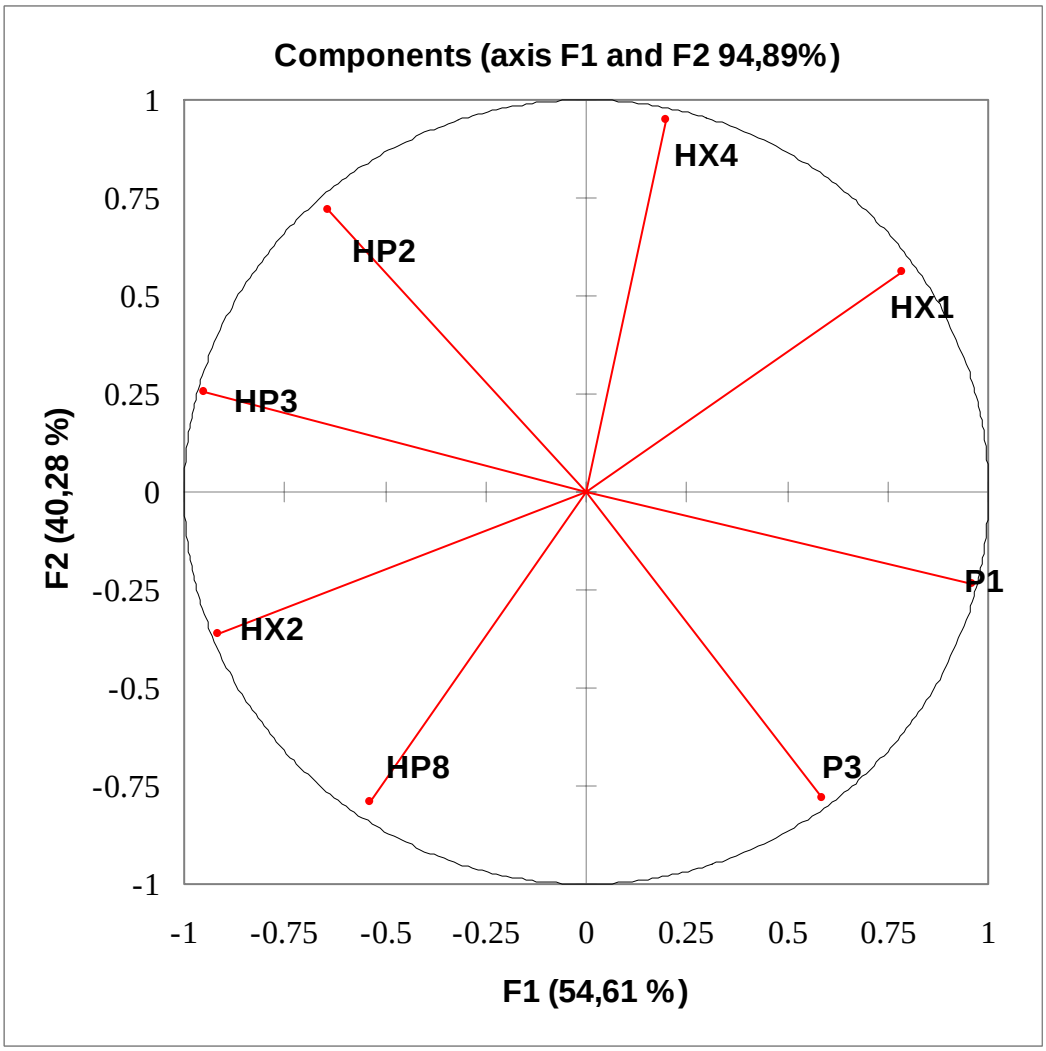
Components (axis F1 and F2 94,89%)
F2 (40,28 %)
F1 (54,61 %)
1
0.75
0.5
0.25
0
-0.25
-0.5
-0.75
-1
-1
-0.75
-0.5
-0.25
0
0.25
0.5
0.75
1
HX4
HP2
HX1
HP3
P1
HX2
HP8
P3

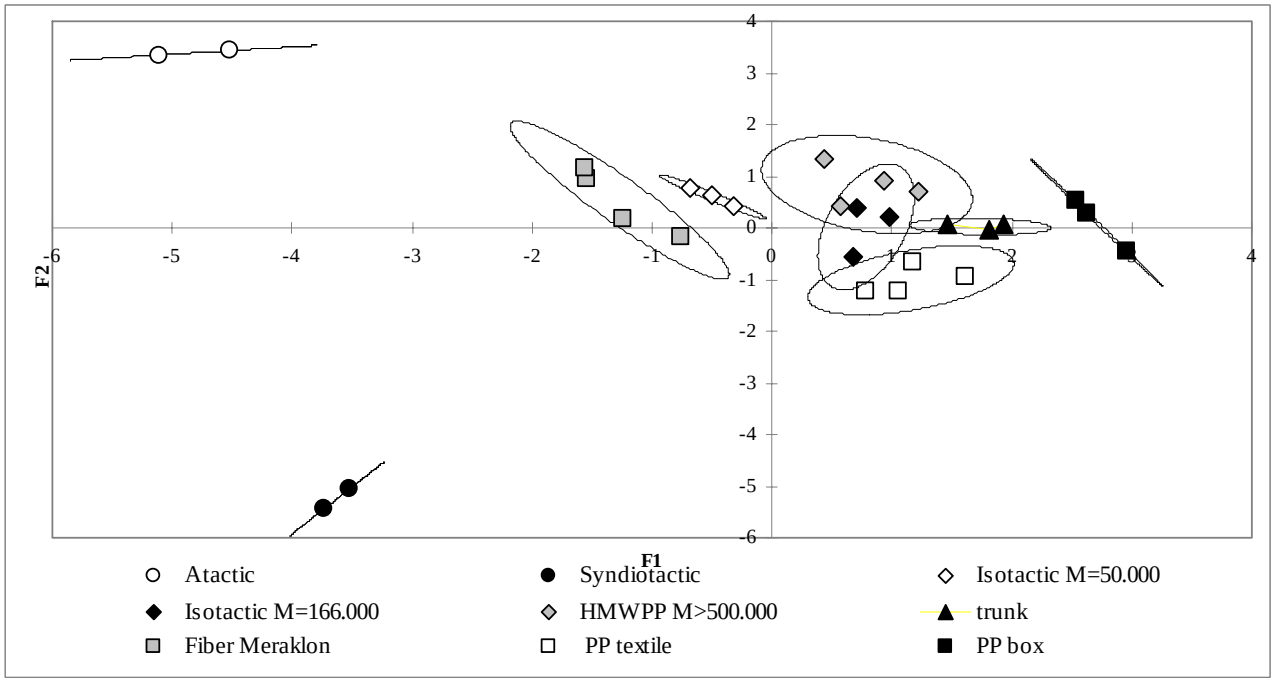
F2
F1
Atactic
Syndiotactic
Isotactic M=50.000
Isotactic M=166.000
HMWPP M>500.000
trunk
Fiber Meraklon
PP textile
PP box

Table 1. Profile of eluition of pentamers (based on ion extraction at m/z 111) and association of peaks ←→ diastereoisomer. The grey circles refers to C^5 where inversion during intramolecular transfer can occur . Enantiomeric forms are not reported

peak	Diastereo isomer	Structure	Group
P1	mm	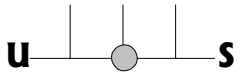	1
P2	mr rm		2 2
P3	rr	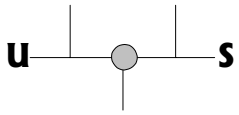	1

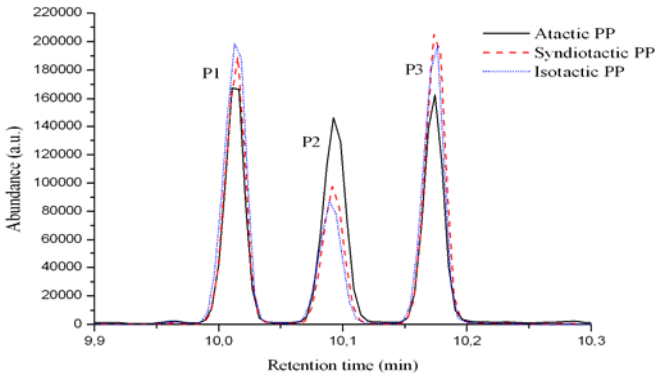

Table 2. Profile of eluition of hexamers (based on ion extraction at m/z 111) and association of peaks ←→ diastereoisomer. The grey circles refer to C^5 an C^9 possibly subjected to inversion during intramolecular transfer. Enantiomeric form are not reported

peak	Diastereo-isomer	Structure	Group

HX1	mmm	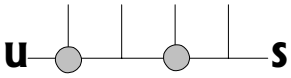	1	
HX2	rmm mmr	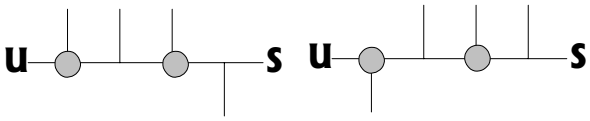	2	1
HX3	mrm rmr	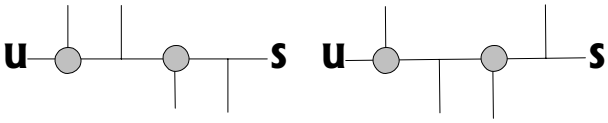	2	2
HX4	mrr rrm	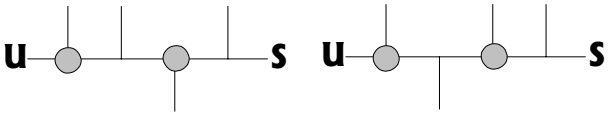	1	2
HX5	rrr	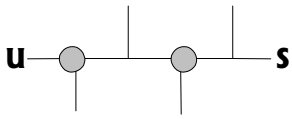	1	

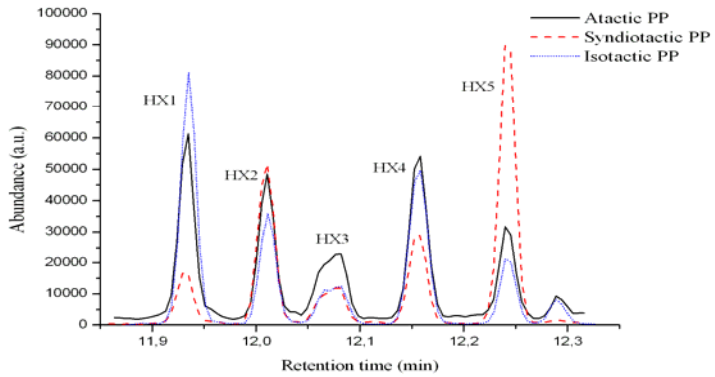

Table 3: Profile of eluition of heptamers (based on ion extraction at m/z 111) and association of peaks ←→ diastereoisomer. The grey circles refer to C5 an C9 that can be subjected to inversion during intramolecular transfer. Enantiomeric form are not reported.

peak	Diastereo-isomer	Structure	Group
HP1	mmmm	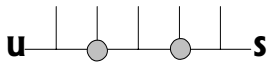	1
HP2	rmmm mmmr	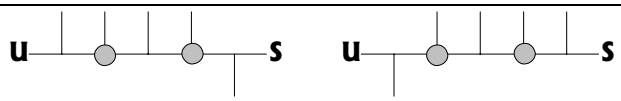	2
HP3	mrmm mmrm		2
HP4	rmmr mrrm mmrr rrmm	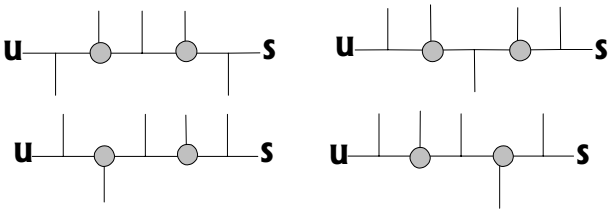	3 1
HP5	rmrm mrmr	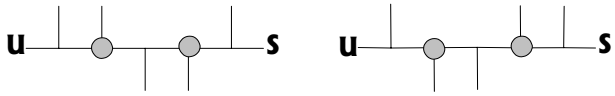	3
HP6	rmrr rrmr	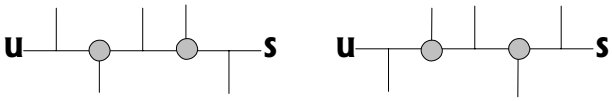	2
HP7	rrrm mrrr	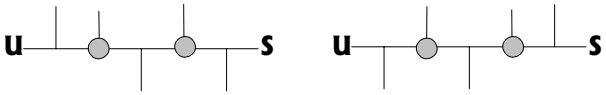	2
HP8	rrrr	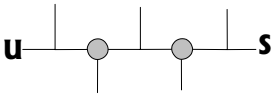	1

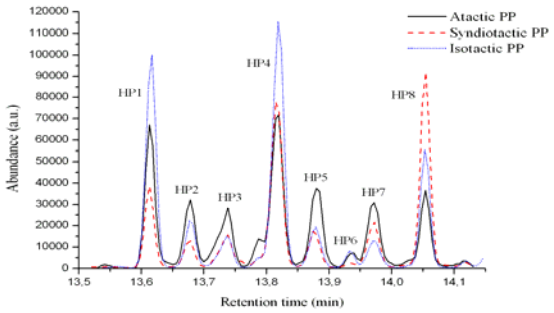

Table 4. Contribute of each component to the variables F1 and F2 of the second PCA

Peak	attribution	F1	F2
P1	iso	0,460	-0,130
P3	syn	0,281	-0,436
HX1	iso	0,376	0,313
HX2	at	-0,437	-0,201
HX4	at	0,096	0,528
HP2	at	-0,308	0,400
HP3	at	-0,455	0,141
HP8	syn	-0,257	-0,442

Additional information

Table A area % of peaks related to main 1-alkenes for all PP investigated and used in the First PCA attempt

		P1	P2	P3	HX1	HX2	HX3	HX4	HX5	HP1	HP2	HP3	HP4	HP5	HP6	HP7	HP8
PP textile	T1	23,02	8,14	20,95	6,03	2,78	1,38	4,47	1,62	9,46	1,51	0,91	12,29	1,52	0,50	0,86	4,58
	T2	23,61	7,77	21,27	6,61	2,63	1,37	4,59	1,60	9,60	1,53	0,80	11,67	1,38	0,57	0,84	4,16
	T3	23,02	8,41	20,97	6,40	2,62	1,49	4,46	1,61	9,30	1,87	0,69	12,09	1,49	0,54	0,83	4,18
	T4	22,58	8,45	20,77	5,91	2,59	1,61	4,37	1,68	9,54	1,60	1,05	11,77	1,55	0,70	1,01	4,83
Meraklon fibre	F1	20,74	8,90	19,29	5,85	3,05	1,73	4,74	1,90	8,78	1,86	1,62	12,52	1,94	0,56	1,39	5,14
	F2	20,12	9,22	18,89	5,76	3,26	1,87	4,88	1,91	8,65	1,94	1,78	12,82	2,09	0,37	1,33	5,13
	F3	19,61	9,38	18,46	6,16	3,32	1,96	5,20	2,07	8,57	2,11	1,90	12,41	2,05	0,41	1,34	5,12
	F4	19,25	8,81	17,84	6,70	3,35	1,88	5,24	2,06	9,22	2,11	1,75	12,58	2,10	0,55	1,30	5,26
Atactic PP	PA1	16,15	15,55	14,99	5,63	4,24	3,17	5,23	2,67	6,35	2,78	3,13	8,93	4,19	0,39	3,10	3,41
	PA2	15,56	15,54	14,68	5,42	4,14	3,23	5,26	2,88	6,65	2,89	3,31	9,11	4,21	0,38	3,36	4,40
Iso PP 50	PI1	22,33	7,89	19,99	6,64	2,75	1,39	4,67	1,61	8,91	1,56	1,18	11,87	1,42	0,46	2,63	4,69
	PI2	21,86	7,49	19,37	7,67	2,71	1,32	4,95	1,63	9,46	1,73	1,12	11,25	1,39	0,79	2,80	4,45
	PI3	22,17	7,30	19,46	7,96	2,74	1,37	4,92	1,61	9,49	1,57	1,11	11,04	1,38	0,79	2,72	4,37
Iso PP 166	PI4	21,43	8,64	18,96	6,73	3,09	1,79	4,95	1,75	9,06	1,82	1,61	11,83	1,87	0,56	1,29	4,62
	PI5	21,04	9,06	18,61	6,89	3,15	1,85	5,03	1,92	8,81	1,86	1,63	11,62	2,03	0,51	1,34	4,66
	PI6	20,59	8,84	18,53	6,91	3,18	1,75	5,11	1,89	9,11	1,94	1,55	11,94	1,89	0,56	1,29	4,91
Syndio PP	PS1	19,41	10,74	21,17	1,70	5,16	1,85	3,24	8,35	3,75	1,37	1,93	9,19	1,87	0,03	2,17	8,05
	PS2	18,85	10,43	21,11	1,75	5,19	1,70	3,21	8,97	3,60	1,25	1,94	8,94	1,85	0,09	2,30	8,82
Trunktapestry	B5	23,49	6,59	20,12	8,77	2,47	1,12	4,93	1,38	10,46	1,47	0,90	10,96	1,12	1,09	0,87	4,25
	B6	23,43	6,64	20,09	8,62	2,53	1,11	4,88	1,44	10,38	1,50	0,89	11,05	1,14	1,05	0,86	4,40
	B7	22,78	6,78	20,03	8,30	2,57	1,16	5,01	1,57	10,17	1,51	1,00	11,34	1,28	0,98	0,98	4,56
PP food box	VAS1	23,67	6,40	19,93	9,79	2,36	0,90	5,03	1,21	11,22	1,44	0,67	10,16	1,02	1,71	0,71	3,78
	VAS2	25,03	6,51	20,87	8,97	2,23	0,99	4,69	1,22	10,67	1,29	0,64	10,13	0,97	1,28	0,73	3,78
	VAS3	24,01	6,31	20,57	9,72	2,33	0,82	4,80	1,16	11,22	1,58	0,62	9,71	1,11	1,72	0,72	3,61
HMW PP	HM1	20,55	7,60	17,42	8,36	2,66	1,12	5,03	1,49	9,61	1,73	0,99	9,47	1,45	1,18	7,27	4,08
	HM2	21,68	7,70	18,72	8,49	2,73	1,10	5,00	1,47	9,85	1,70	1,01	9,89	1,38	1,16	4,21	3,92
	HM3	21,97	7,51	19,11	8,52	2,62	1,09	5,01	1,50	10,03	1,61	0,96	10,13	1,35	1,04	3,56	4,00
	HM5	21,59	8,11	19,15	7,39	2,79	1,30	5,00	1,70	9,30	1,66	1,15	10,70	1,55	0,69	3,52	4,41

Table B. End groups of products of thermal degradation of PP from ref 15

End groups

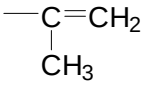
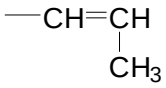
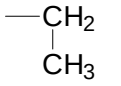

Table C Structure of the main products of thermal degradation of PP found in our pyrolysis tests

End group 1	End group 2	%* (typical)	formula	MW
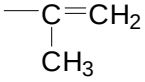	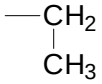	53-67	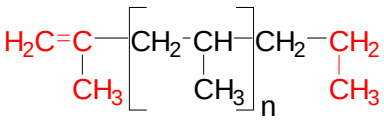	n=0: 84; n=1: 126; n=2: 168; n=3: 210; n=4: 252; n=5: 294.
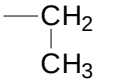	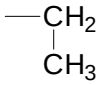	9-10	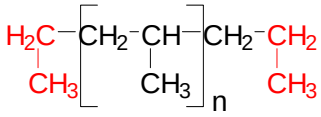	n=0: 72; n=1: 114; n=2: 156.
	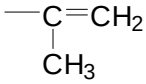	4-6	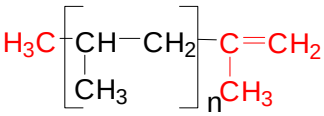	n=0: 56; n=1: 98; n=2: 140; n=3: 182; n=4: 224; n=5: 266.
		3-4	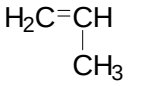	42
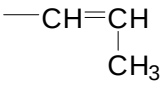	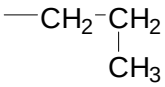	1-2	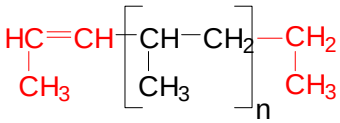	n=0: 70; n=1: 112; n=2: 154
	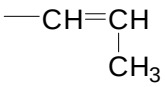	<1	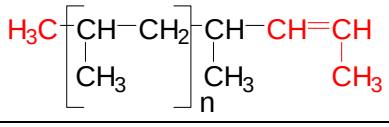	n=0: 84; n=1: 126; n=2: 168; n=3: 210; n=4: 252; n=5: 294..
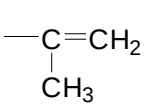	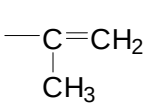	<1	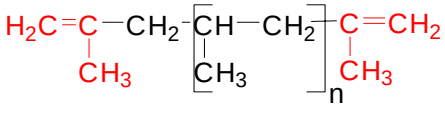	n=0: 96; n=1: 138; n=2: 180; n=3: 222; n=4; 264; n=5: 306..

* calculated on the basis of integration of Total Ion Chromatogram signal, TIC.

Table D MS spectra of main and some minor pyrolysis product and their mechanism of formation

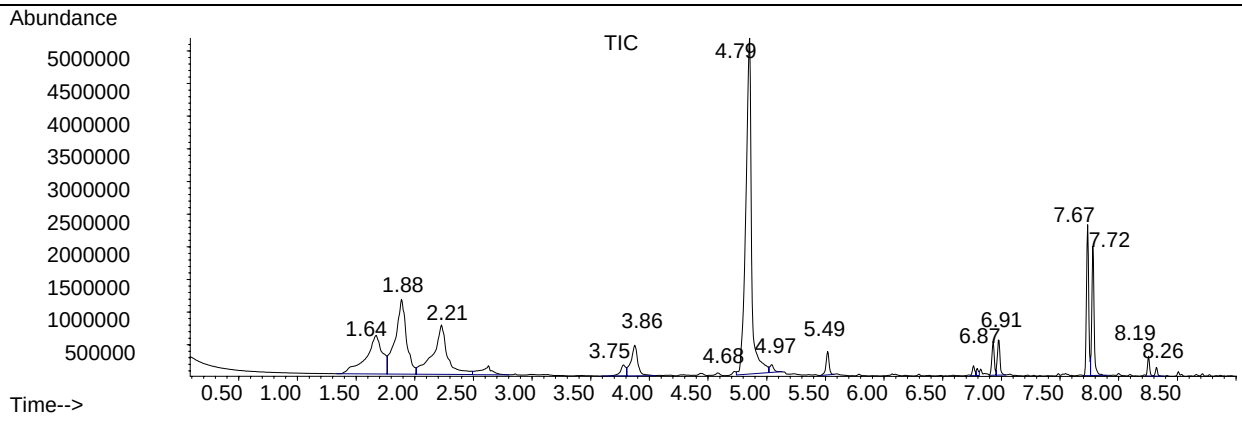

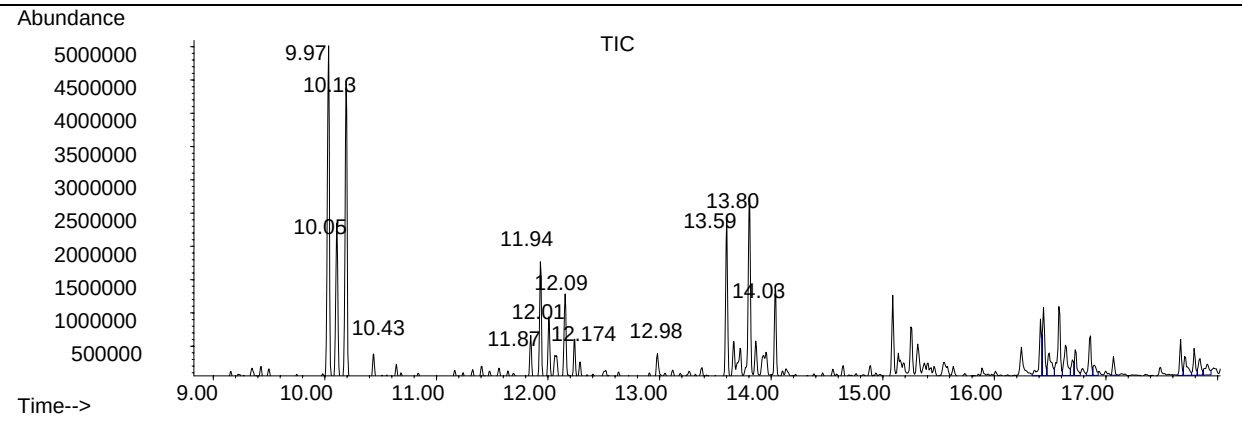

MS spectrum	Formula MW mechanism of formation
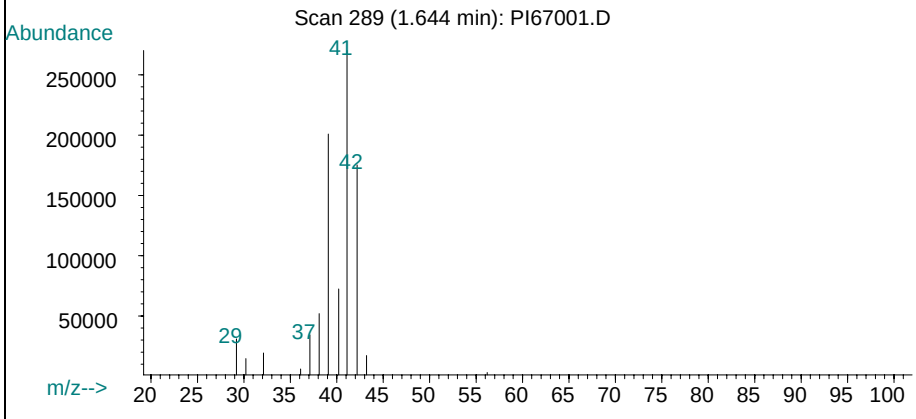	$CH_2=CH(CH_3)$ C_3H_6 42 depolymerization

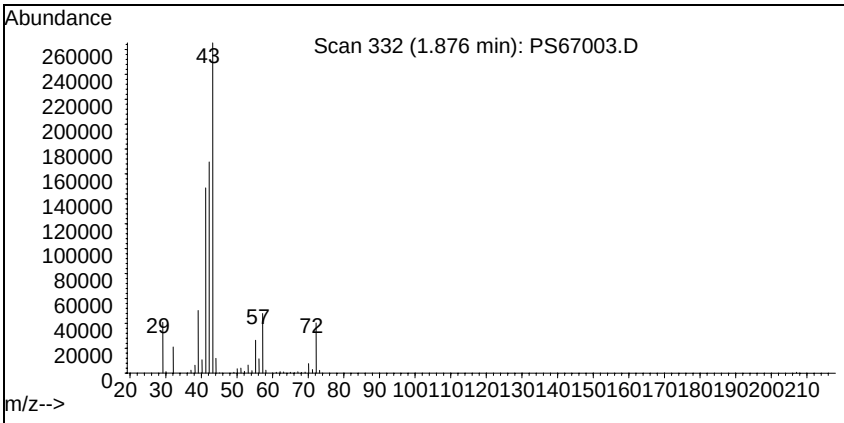

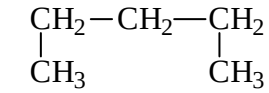

C_5H_{12}

72

intramolecular H transfer 1→5 from R2, right b scission

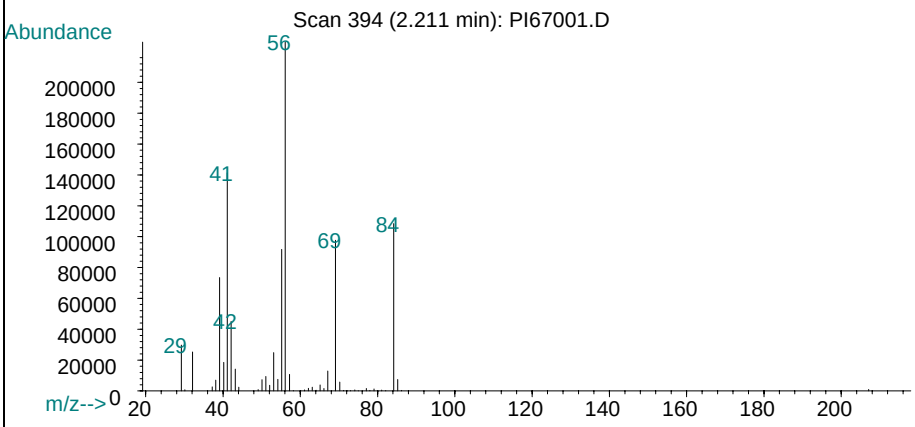

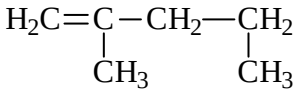

C_6H_{12}

84

intramolecular H transfer 1→3from R2, link β scission

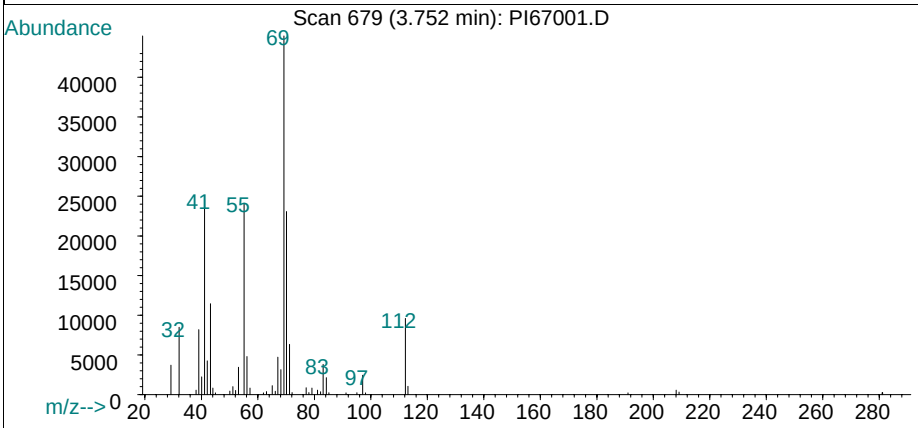

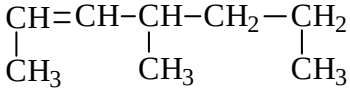

C_8H_{16}

112

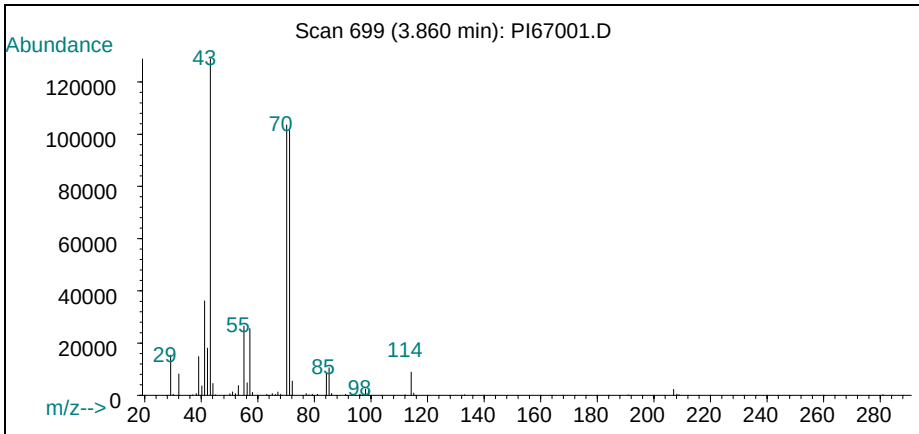

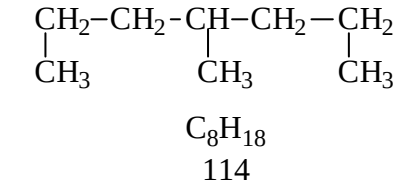

C_8H_{18}
114

intramolecular H transfer 1→5→3 from R2, right β scission

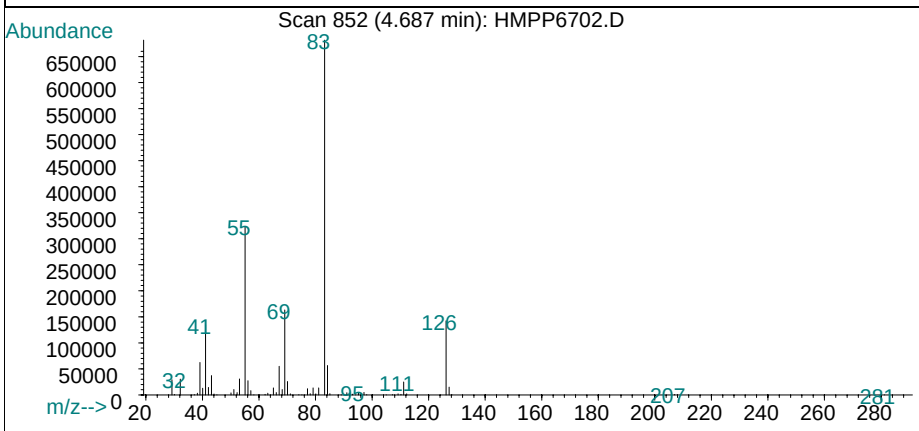

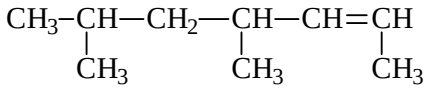

C_9H_{18}
126

intramolecular H transfer 1→5 from R2, link β scission

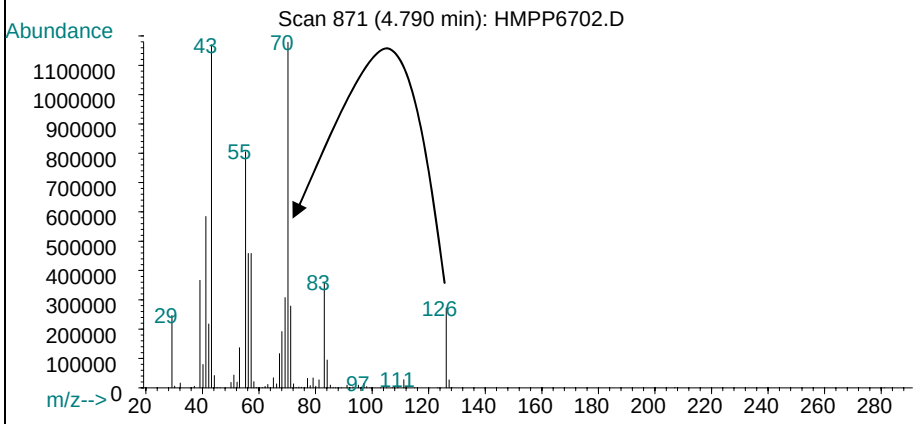

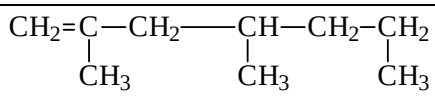

C_9H_{18}
126

intramolecular H transfer 1→5 from R2, link β scission

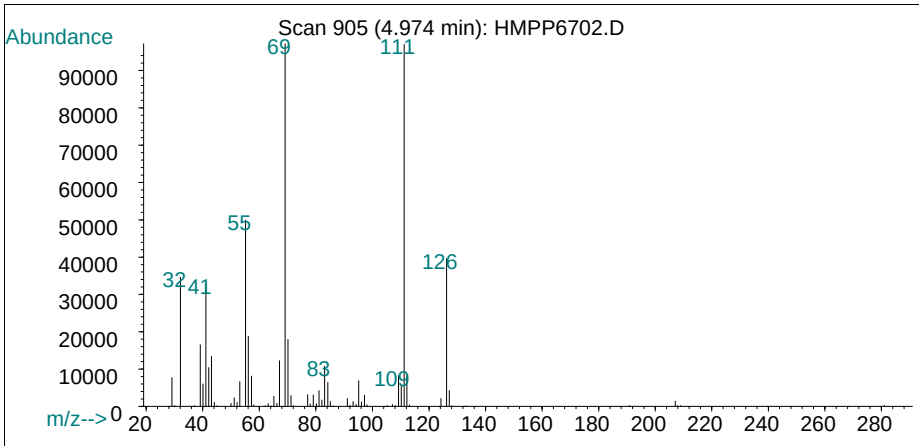

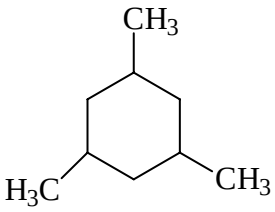

C_9H_{18}
126

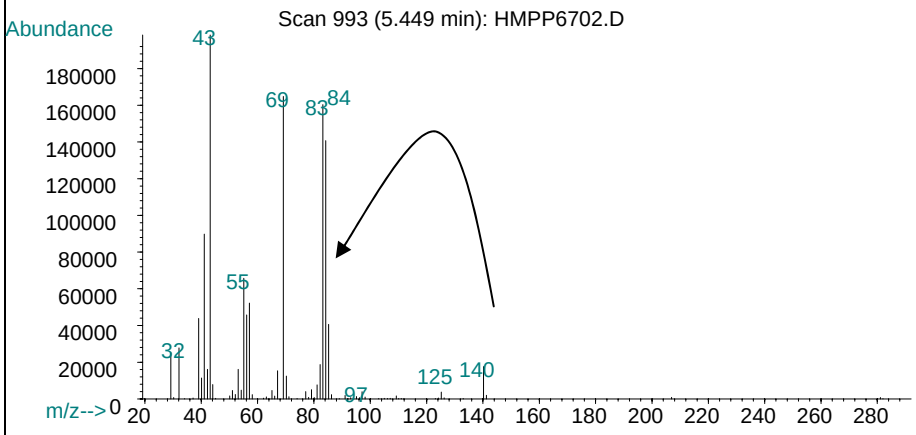

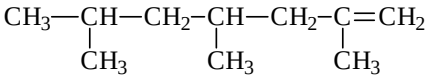

$C_{10}H_{20}$
140

intramolecular H transfer 1→6 from R1, link β scission

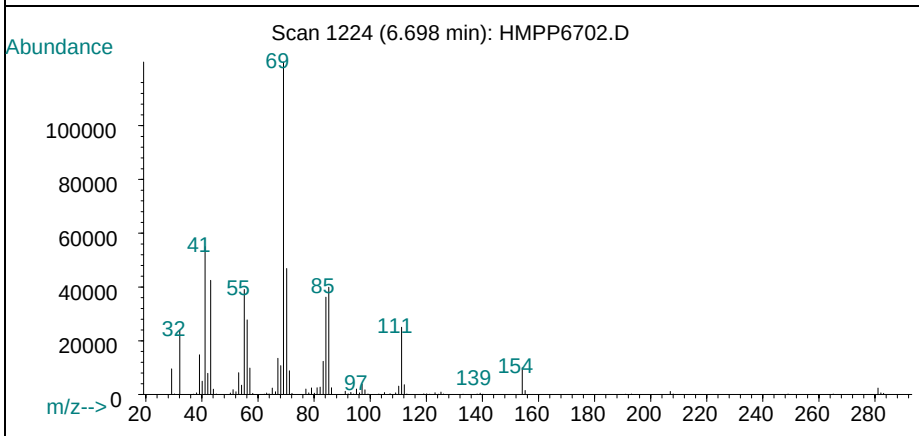

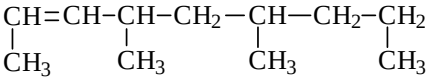

$C_{11}H_{22}$
154

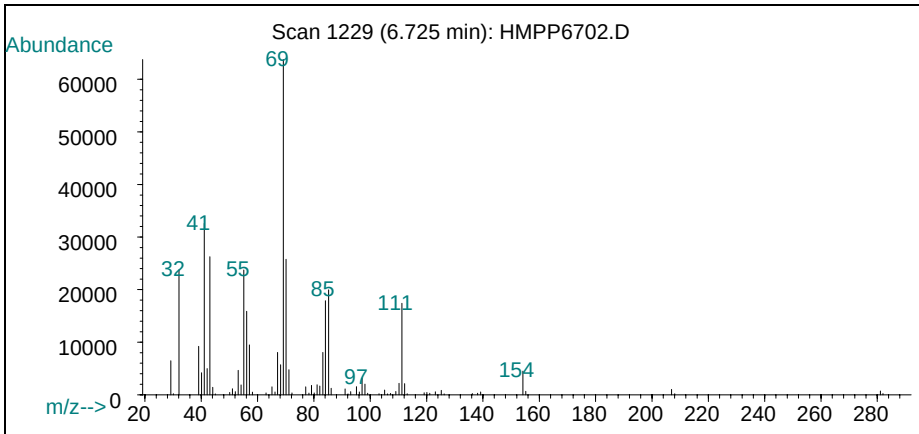

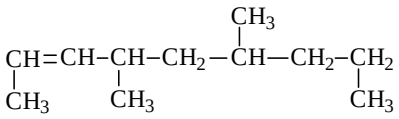

$C_{11}H_{22}$
154.29

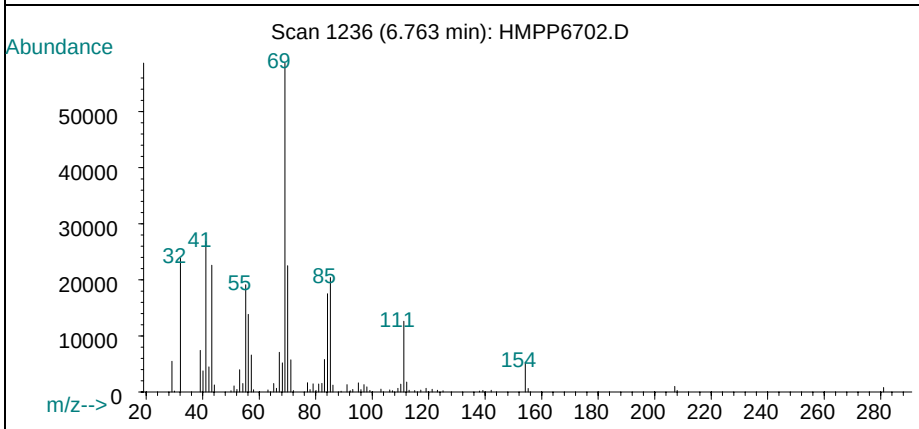

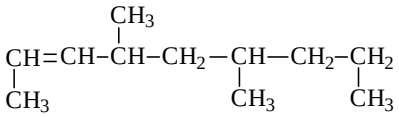

$C_{11}H_{22}$
154.29

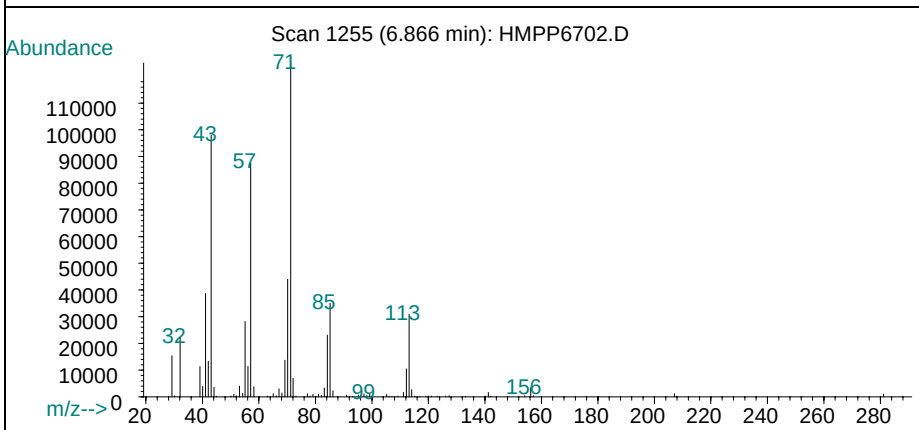

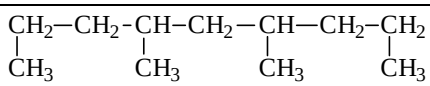

$C_{11}H_{24}$
156

intramolecular H transfer 1→5→5
from R2, right β scission

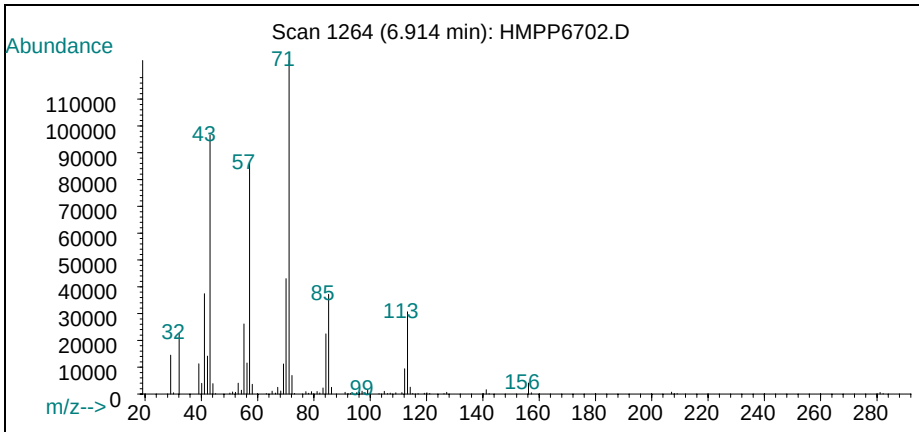

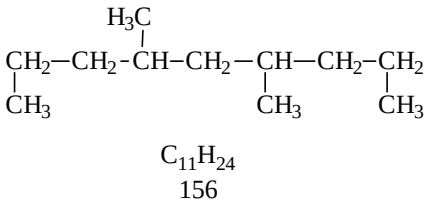

$C_{11}H_{24}$
156

intramolecular H transfer 1→5→5
from R2, right β scission

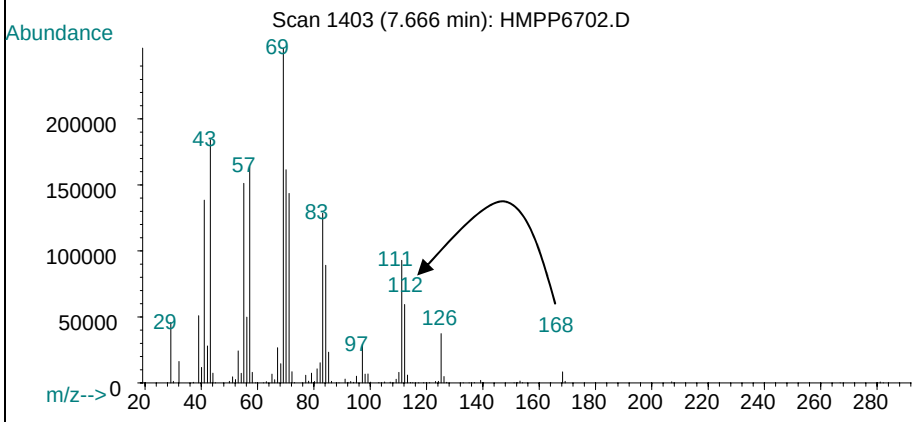

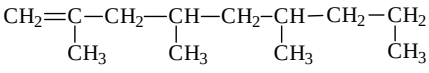

$C_{12}H_{24}$
168

intramolecular H transfer 1→5→3
from R2, link β scission

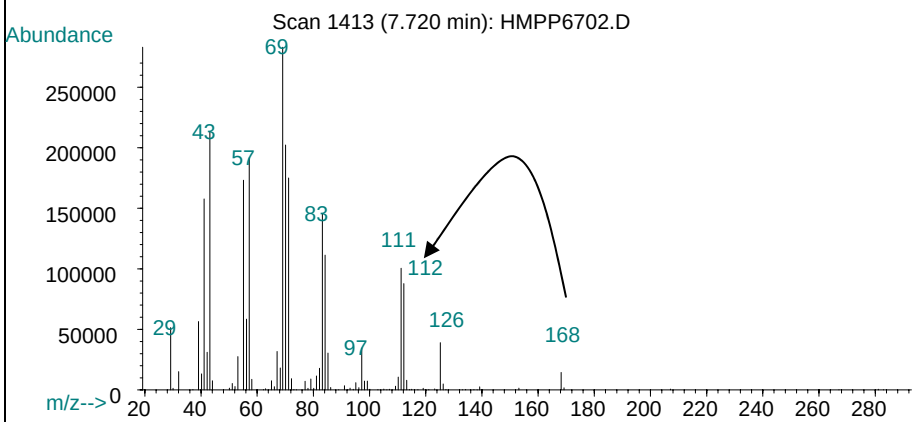

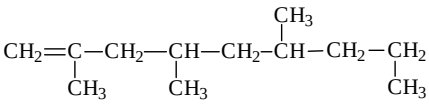

$C_{12}H_{24}$
168

intramolecular H transfer 1→5→3
from R2, link β scission

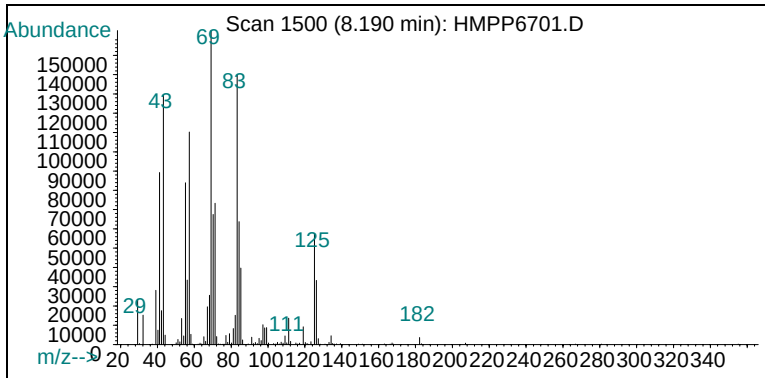

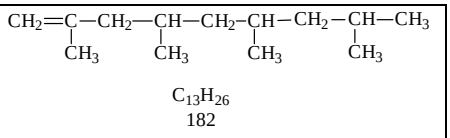

$C_{13}H_{26}$
182

intramolecular H transfer 1→6→3
from R1, link β scission

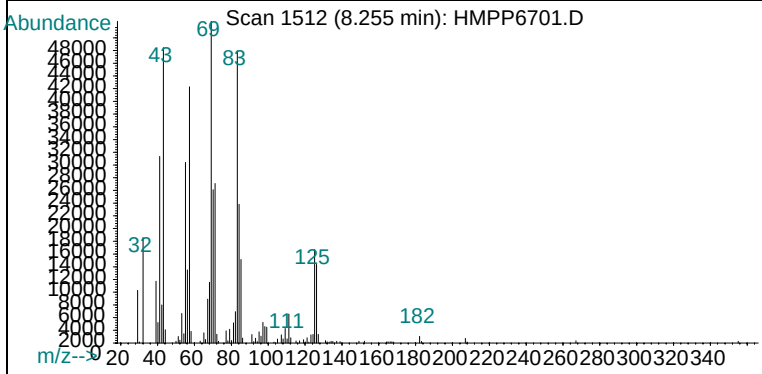

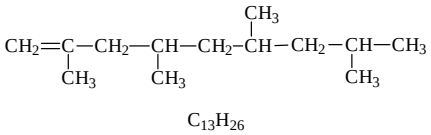

$C_{13}H_{26}$
182.203450

intramolecular H transfer 1→6→3
from R1, link β scission

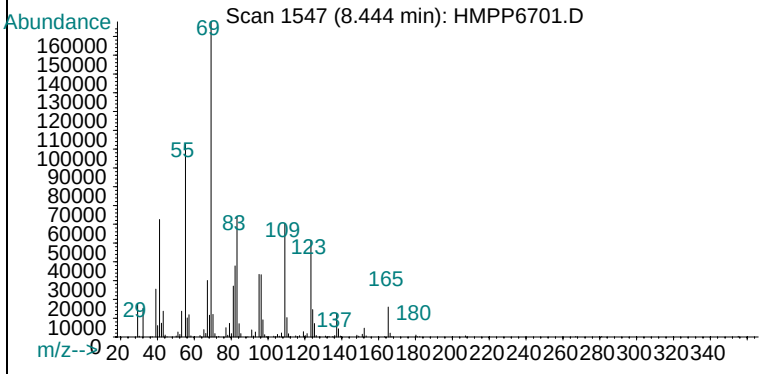

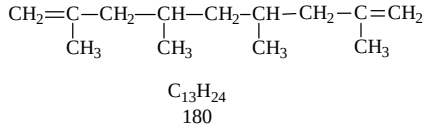

$C_{13}H_{24}$
180

disproportionation

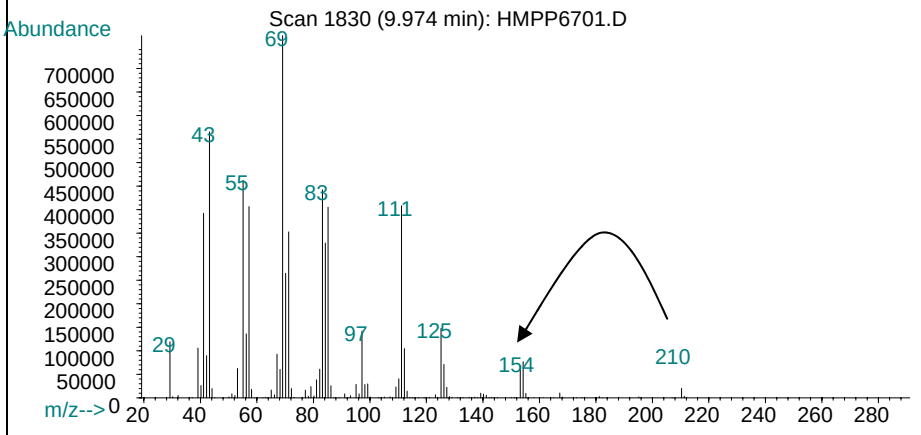

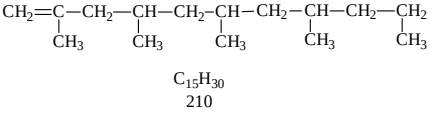

$C_{15}H_{30}$
210

intramolecular H transfer 1→5→5
from R2, link β scission

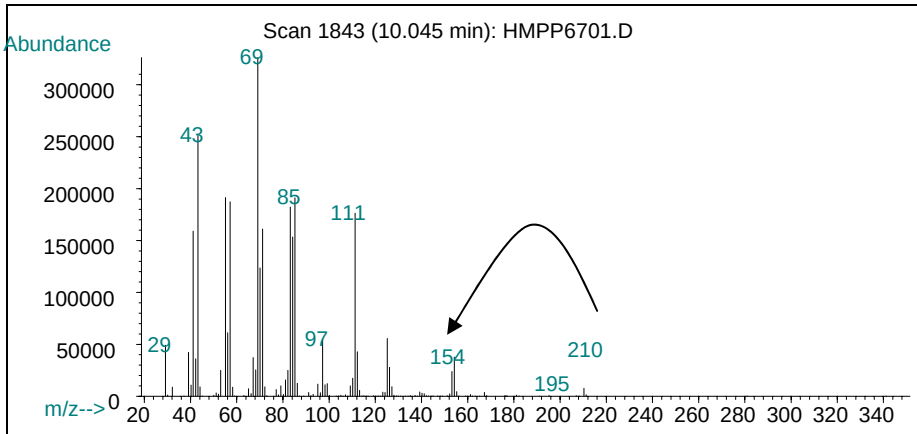

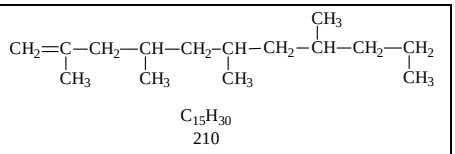

$C_{15}H_{30}$
210

intramolecular H transfer 1→5→5
from R2, link β scission

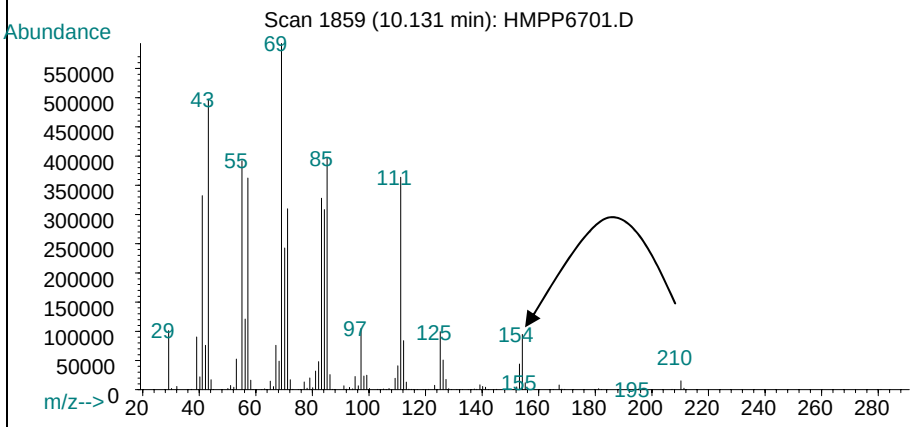

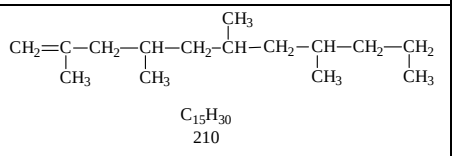

$C_{15}H_{30}$
210

intramolecular H transfer 1→5→5
from R2, link β scission

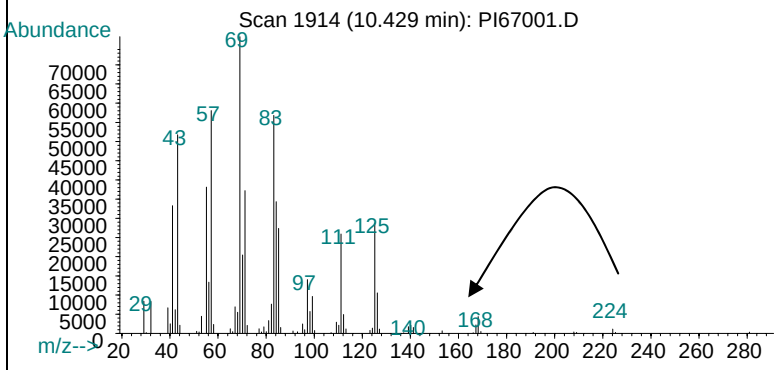

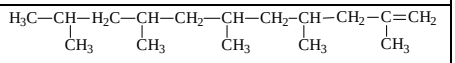

$C_{16}H_{32}$
224

intramolecular H transfer 1→6→5
from R1, link β scission

<table>
<tr>
<td> 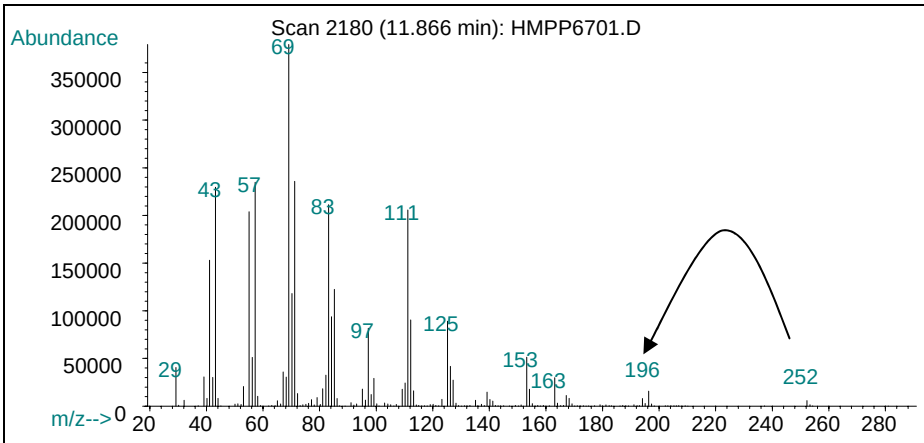
</td>
<td> 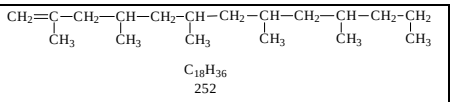

intramolecular H transfer
1→5→5→3 from R2, link β scission</td>
</tr>
<tr>
<td>Retention times 11.94, 12.01, 12.09, 12.17</td>
<td>Isomers of the previous one according to table 2 in the text</td>
</tr>
<tr>
<td> 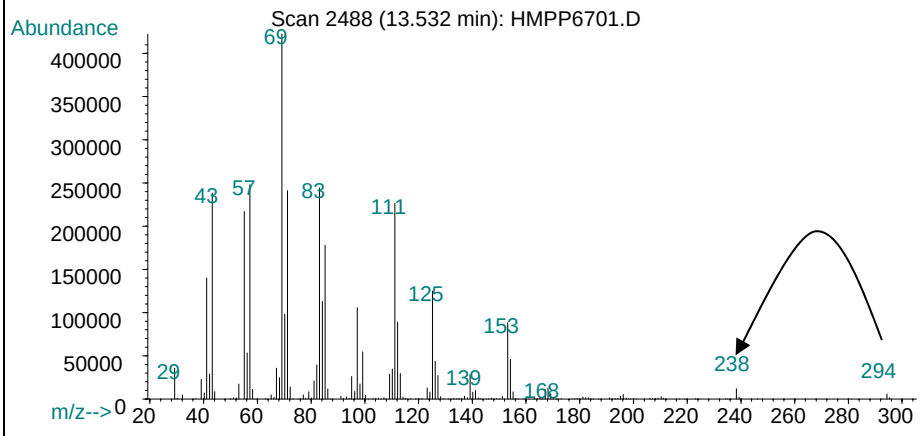
</td>
<td> 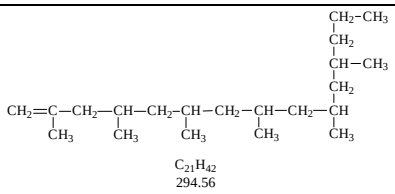

intramolecular H transfer
1→5→5→5 from R2, link β scission</td>
</tr>
<tr>
<td>Retention times 13.66, 13.74, 13.80, 13.88, 13.97 13.95, 14.03</td>
<td>Isomers of the previous one according to table 3 in the text</td>
</tr>
</table>